TID/SNA--2047

MASTER

RESEARCH REPORT

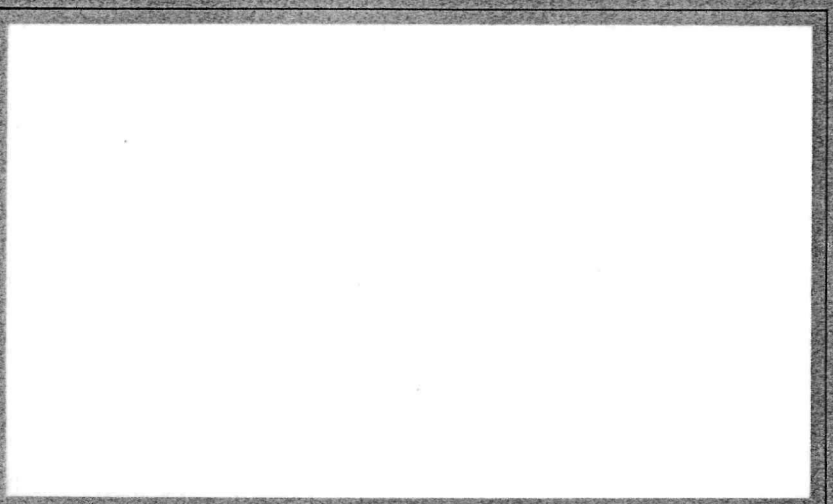

Battelle
Columbus Laboratories

DISCLAIMER

TID/SNA--2047

MASTER

FINAL REPORT

on

LOW-CYCLE FATIGUE OF TYPE 347 STAINLESS STEEL AND HASTELLOY X IN HYDROGEN GAS ENVIRONMENT

to

AEROJET NUCLEAR SYSTEMS COMPANY

December 20, 1971

by

C. E. Jaske and T. L. Porfilio

TABLE OF CONTENTS

LIST OF TABLES

LIST OF TABLES
(Continued)

LIST OF FIGURES

LIST OF FIGURES
(Continued)

LIST OF FIGURES
(Continued)

LIST OF SYMBOLS

A_T - Area of specimen at temperature, $in.^2$

D_T - Minimum specimen diameter at temperature, in.

E - Modulus of elasticity, ksi

K - Compliance constant, lb^{-1}

N_0 - Number of cycles to detectable cracking

N_5 - Number of cycles to significant cracking

N_f - Number of cycles to total fracture

P - Load on specimen, lb

ΔP - Load range, lb

S - Stress, ksi

ΔS - Stress range, ksi

$\dot{\epsilon}$ - Axial strain rate

ϵ_d - Diametral strain

ϵ_{de} - Elastic component of diametral strain

$\Delta\epsilon_{de}$ - Change in elastic component of diametral strain

ϵ_p - Plastic component of axial strain

ϵ_t - Total axial strain

$\Delta\epsilon_t$ - Total axial strain range

ν_e - Poisson's ratio, elastic

ν_p - Poisson's ratio, plastic

LOW-CYCLE FATIGUE OF TYPE 347 STAINLESS STEEL AND HASTELLOY X IN HYDROGEN GAS ENVIRONMENT

by

C. E. Jaske and T. L. Porfilio

SUMMARY

An experimental investigation has been conducted to assess the low-cycle fatigue resistance of two alloys, Type 347 stainless steel and Hastelloy X, that are being considered for use in nuclear-powered rocket vehicles. Constant-amplitude, strain-controlled low-cycle fatigue tests were conducted under compressive strain cycling at a constant strain rate of 10^{-3} sec^{-1}. Specimens were tested in a purified hydrogen gas environment at temperatures of 1000, 1400, and 1600 F.

Specimens were obtained from three heats of Type 347 stainless steel bar and two heats of Hastelloy X bar. At each temperature, low-cycle fatigue tests were conducted at total strain ranges of 1.5, 3.0, and 5.0 percent. Three replicates of each test condition were used for each heat of Type 347 stainless steel and four replicates were used for each heat of Hastelloy X. Information on cyclic hardening and/or softening behavior was developed for both alloys at all three temperatures. Total, elastic, and plastic strain range versus fatigue life curves were developed for each of the five heats of material at each of the three temperatures.

INTRODUCTION

During the operation of nuclear-powered rocket engines, some areas of the rocket nozzle will be exposed to hydrogen gas and subjected to temperature fluctuations of sufficient magnitude to produce large cyclic compressive thermal strains. Since these cyclic strains may produce fatigue cracks or failures in less than 1,000 cycles, it is important to consider the low-cycle fatigue resistance of materials to be used in this application. This program was undertaken to develop comparative low-cycle-fatigue design information for two such materials, Type 347 stainless steel and Hastelloy X.

To accomplish this objective, strain-controlled low-cycle fatigue tests of both these alloys were conducted in a hydrogen gas environment at

temperatures of 1000, 1400, and 1600 F. In addition to the low-cycle fatigue tests conducted in a hydrogen atmosphere, tensile and low-cycle fatigue tests were also performed in air to establish basic mechanical properties. The tensile tests were conducted in air at 70, 1000, 1200, and 1400 F; the low-cycle-fatigue tests were in air at 1400 F.

EXPERIMENTAL PROCEDURE

All material used in this program was furnished by Aerojet Nuclear Systems Company (ANSC) in the form of 3/4-inch diameter bar stock that had undergone heat treatment cycles to simulate brazing operations actually used in fabrication of the nozzle. Bar stock was from three different heats of Type 347 stainless steel and two different heats of Hastelloy X.

Microstructure

To determine the typical microstructure of the materials used in this program, both longitudinal and transverse metallurgical samples were taken from each heat of material. These samples were mounted, polished, and etched for visual examination. The Type 347 stainless steel was etched with a 30HCl, 10HNO_3 solution, and the Hastelloy X was etched with an aqua regia solution. After visual examination, photomicrographs were taken to show the typical microstructure. (See Figures 1 through 5).

Grain sizes of the Type 347 stainless steel samples were estimated using a comparison procedure in accordance with ASTM Designation E-112 (see Table 1). For all three heats, the longitudinal grain size is slightly smaller than the transverse. Heats G-5617 (with specimen prefix B) and G-4943 (with specimen prefix C) have the same grain size, and the material from Heat X-11585 (with specimen prefix A) has a slightly smaller grain size.

Grain sizes of the Hastelloy X samples were estimated using both a comparison procedure (as was the Type 347 stainless steel) and an intercept procedure in accordance with the previously mentioned standard (see Table 1). Because of the presence of some rather small grains, the estimates made by the comparison procedure tended to overestimate the grain size. Thus, the estimates determined by the intercept method were probably more indicative

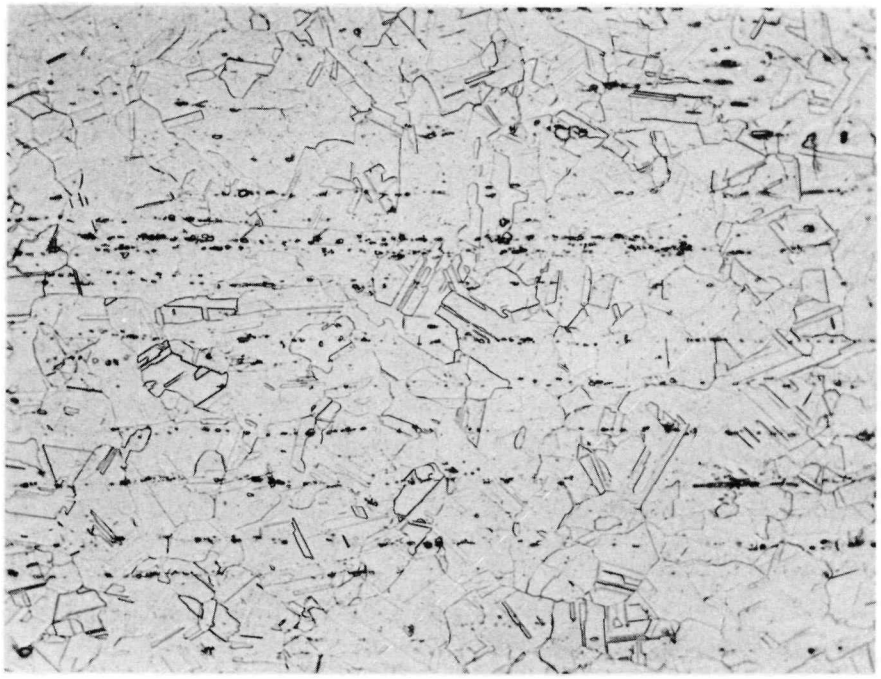

250X 1F051

a. Longitudinal

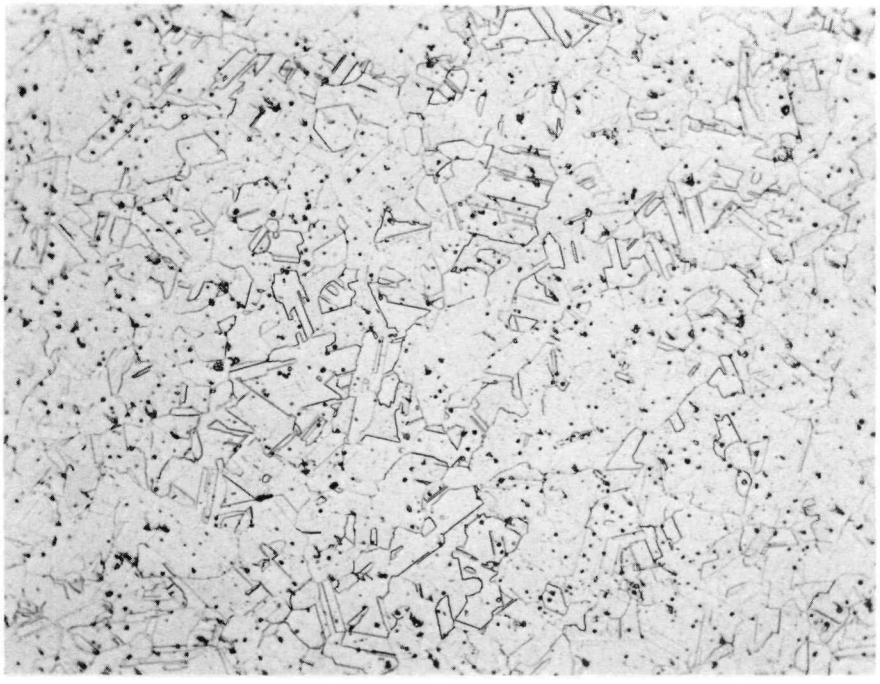

250X 1F050

b. Transverse

FIGURE 1. MICROSTRUCTURE OF HEAT X-11585 OF AISI 347 STAINLESS STEEL AFTER SIMULATED BRAZING (SAMPLES ETCHED WITH 30HCl, 10HNO_3 SOLUTION)

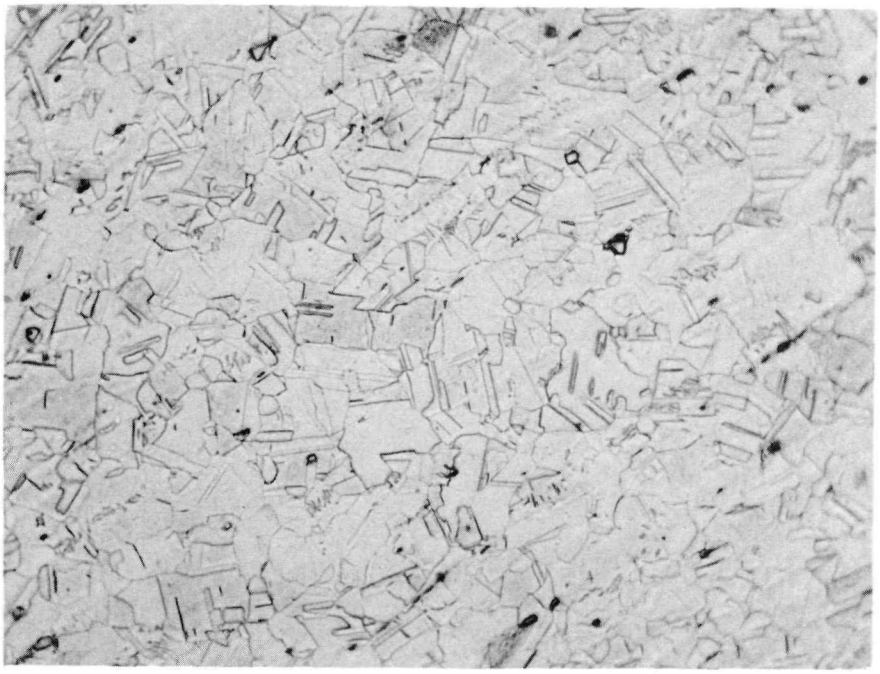

250X 1F053

a. Longitudinal

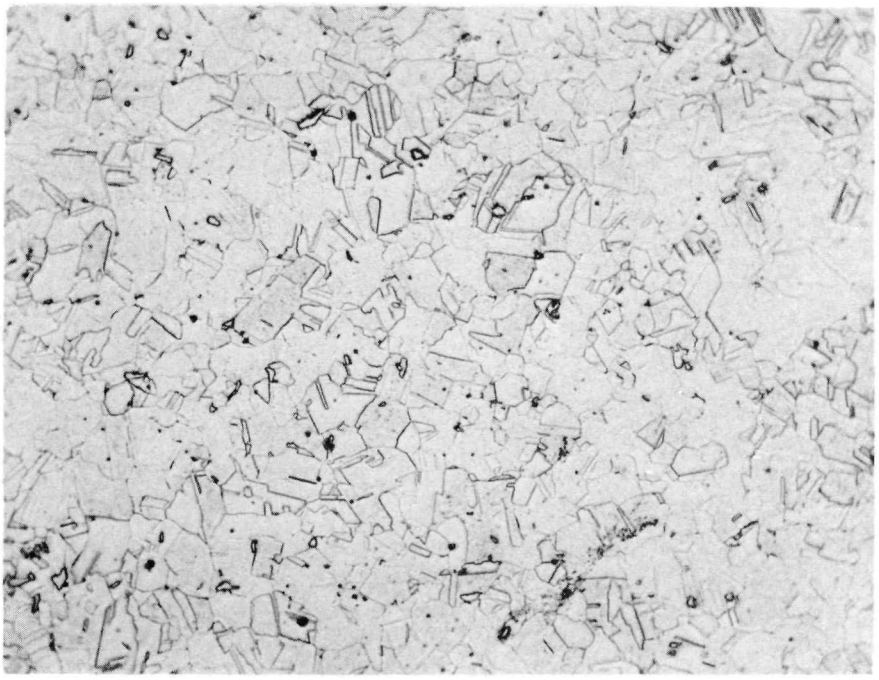

250X 1F052

b. Transverse

FIGURE 2. MICROSTRUCTURE OF HEAT G-5617 OF AISI 347 STAINLESS STEEL AFTER SIMULATED BRAZING (SAMPLES ETCHED WITH 30HC1, 10HNO_3 SOLUTION)

250X 1F055

a. Longitudinal

250X 1F054

b. Transverse

FIGURE 3. MICROSTRUCTURE OF HEAT G-4943 OF AISI 347 STAINLESS STEEL AFTER SIMULATED BRAZING (SAMPLES ETCHED WITH 30HC1, 10HNO_3 SOLUTION)

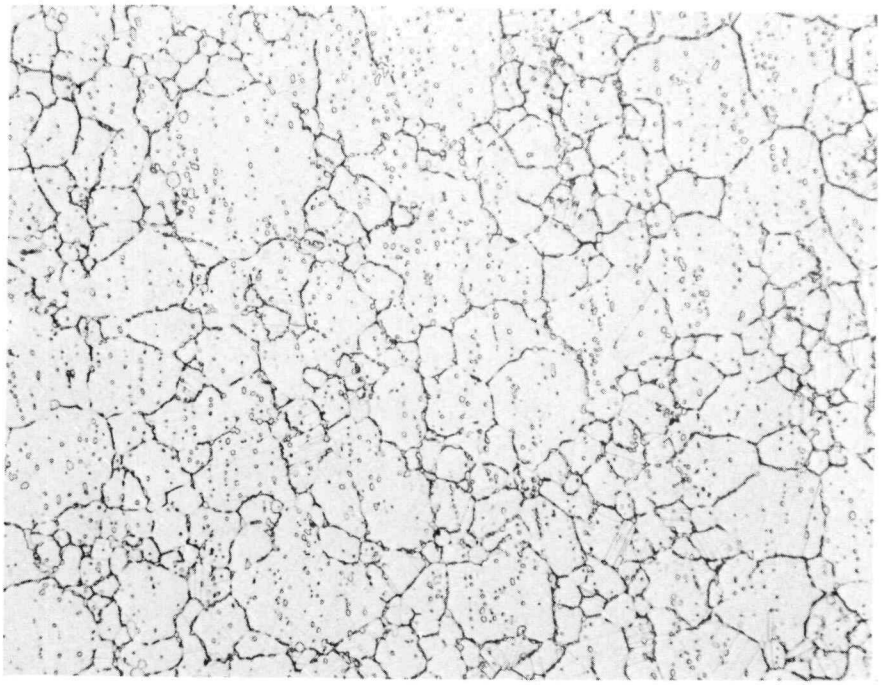

250X 3F281

a. Longitudinal

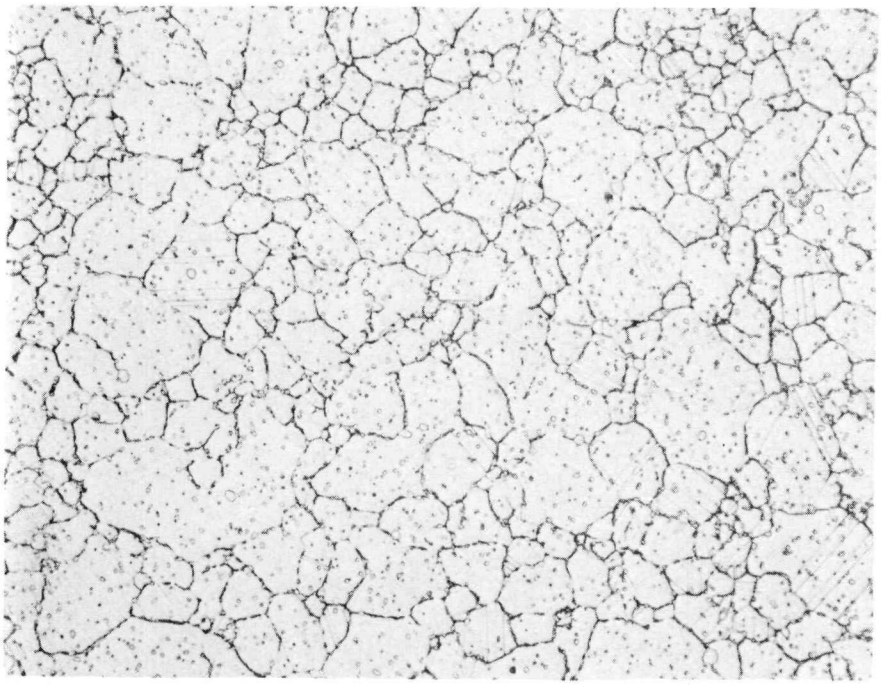

250X 3F279

b. Transverse

FIGURE 4. MICROSTRUCTURE OF HEAT 2610-0-4007 OF HASTELLOY X AFTER SIMULATED BRAZING (SAMPLES ETCHED WITH AQUA REGIA SOLUTION)

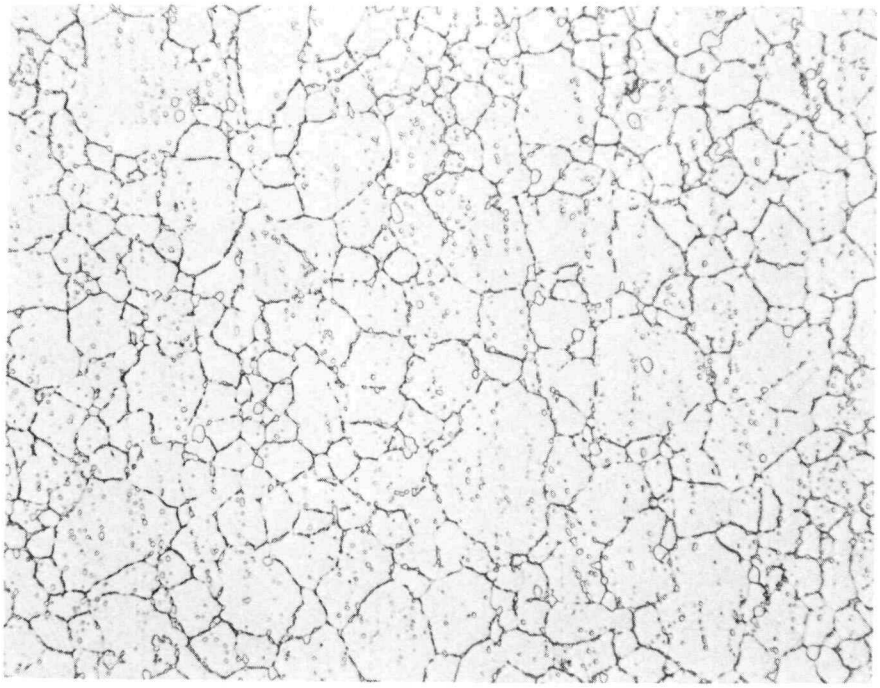

250X 3F282

a. Longitudinal

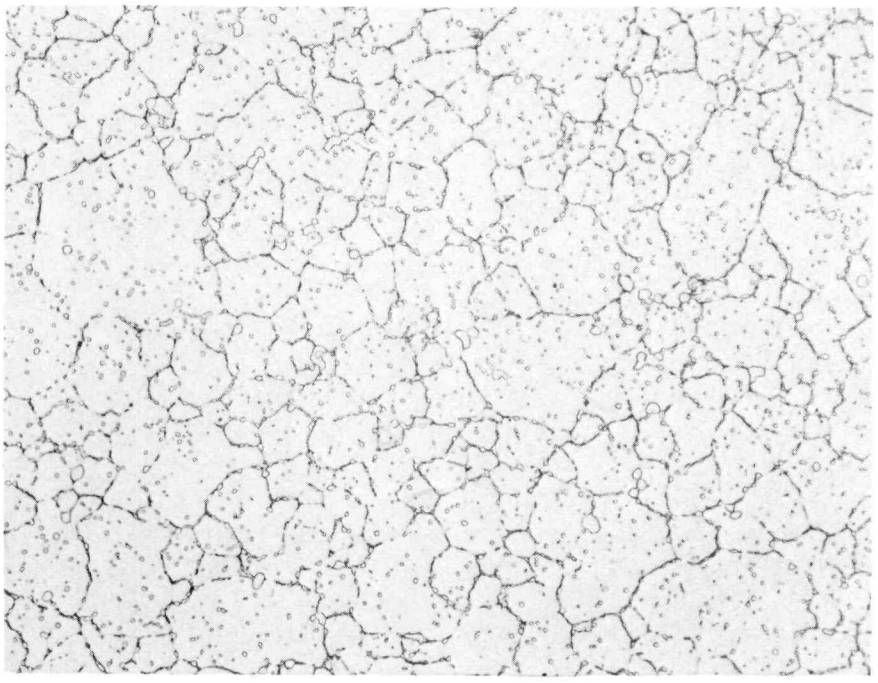

250X 3F280

b. Transverse

FIGURE 5. MICROSTRUCTURE OF HEAT 2610-0-4008 OF HASTELLOY X AFTER SIMULATED BRAZING (SAMPLES ETCHED WITH AQUA REGIA SOLUTION)

TABLE 1. ESTIMATED GRAIN SIZES, AFTER SIMULATED BRAZING OPERATION, FOR AISI 347 STAINLESS STEEL AND HASTELLOY X (IN ACCORDANCE WITH ASTM DESIGNATION: E-112)

Heat	Alpha Code	ASTM Grain Size Number by Comparison Procedure Longitudinal	Transverse	by Intercept Procedure Longitudinal	Transverse
		Type 347 Stainless Steel			
X-11585	A	7.5	7	--	--
G5617	B	8.5	8	--	--
G4943	C	8.5	8	--	--
		Hastelloy X			
2610-0-4007	D	6 to 6.5	6 to 6.5	7.3	7.6
2610-0-4008	E	6 to 6.5	6 to 6.5	7.9	7.1

of the actual average grain size. For the Hastelloy X, there was no significant variation in grain size as either a function of heat or orientation.

Specimen Preparation

Specimens were machined to the configurations shown in Figure 6. The test section of each low-cycle fatigue specimen was polished with successively finer grades of silicon carbide paper to produce a surface finish of 16 μin. rms or better, with finishing marks parallel to the longitudinal axis of the specimen. All specimens were penetrant inspected in accordance with MIL-I-6866, Type I, Method B.

After completing all machining operations, the specimens were degreased with trichlorethylene, followed by reagent acetone. Immediately prior to installation in the test system the specimens were recleaned with a reagent grade acetone.

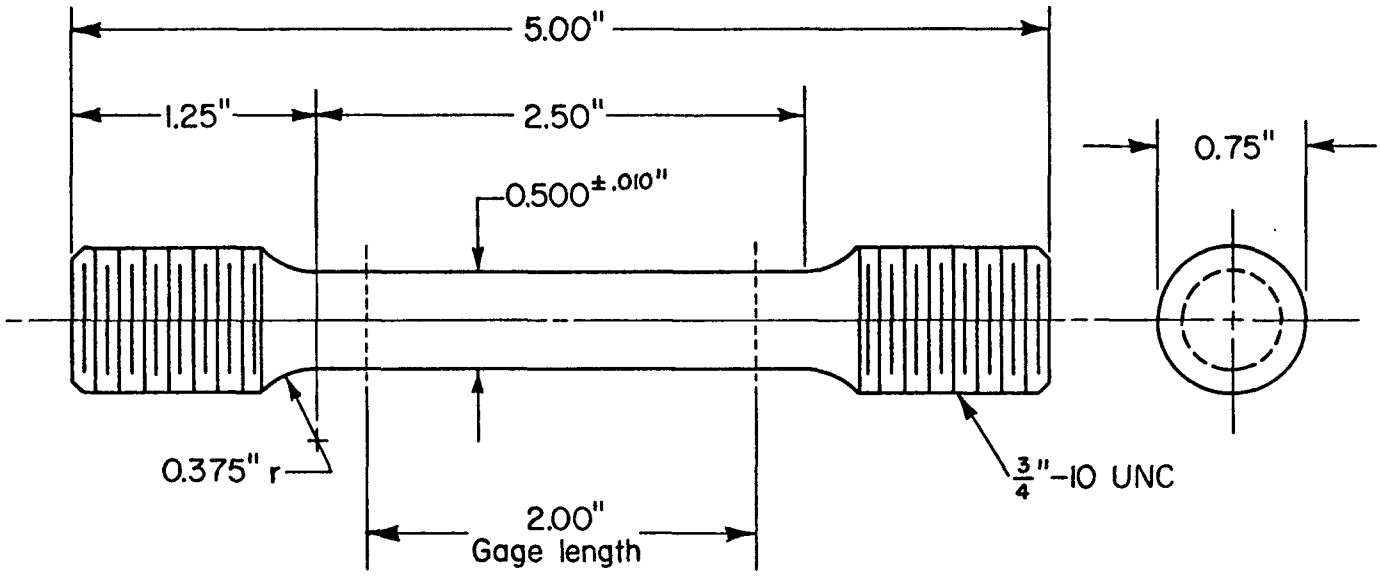

(a) Tensile Specimen

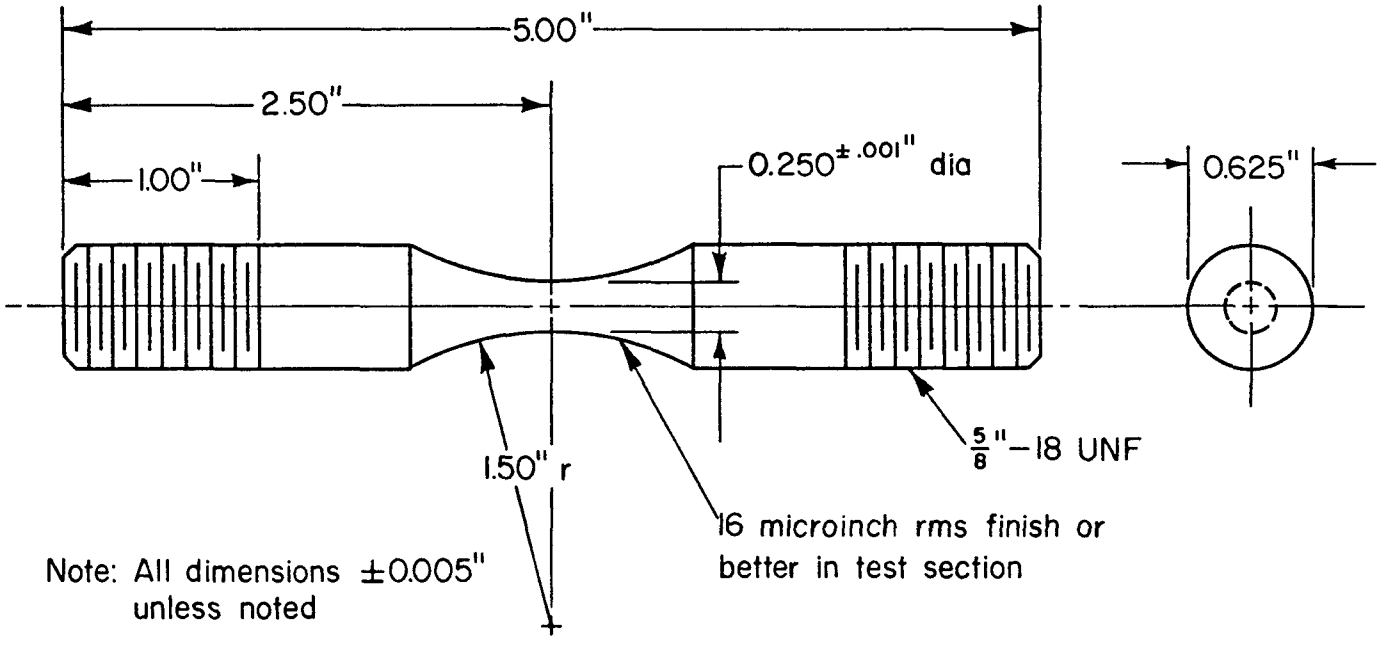

(b) Low-Cycle Fatigue Specimen

A-1110

FIGURE 6. SPECIMEN CONFIGURATIONS

Tensile Apparatus

All of the tensile tests were conducted at a constant strain rate of 0.005 $min.^{-1}$ using a standard hydraulic universal testing machine. Specimens were brought up to and held at temperature by an electrical-resistance heating furnace. Room-temperature tests were conducted in accordance with the methods described in ASTM Designation E8, "Tensile Testing of Metallic Materials", and elevated-temperature tests were performed in accordance with the procedures of ASTM Designation E21, "Short-Time Elevated-Temperature Tension Tests of Materials".

Low-Cycle Fatigue Apparatus

For the low-cycle fatigue experiments, axial load was applied to the specimen using a servocontrolled, electrohydraulic system operated in closed-loop axial strain control (see Figure 7). Diametral changes in the specimen were measured with a special diametral extensometer, and load was measured with a strain-gaged load cell in series with the specimens. Diametral strain and load signals were combined and converted to an equivalent axial strain using an analog computer.[(1)*] Computed axial strain was programmed to follow a fully compressive triangular waveform (see Figure 8a) with a constant axial strain rate of 10^{-3} sec^{-1}. Because of large plastic deformations at the total strain ranges used in this study, the corresponding stress cycles were essentially fully reversed as illustrated in Figure 8b. Calibration of the equipment was in accordance with MIL-C-45662.

The extensometer consists of adjustable sensing arms of high-purity alumina connected to a bracket consisting of two parallel beams joined by a flexible ligament that acts as an elastic hinge. Diameter changes are mechanically multiplied by a factor of three before they are measured at the other end of the extensometer by a sensitive and magnetically shielded linear variable differential transformer (LVDT). The transformer and armature of the LVDT are mounted on opposite beams and the position of the armature relative to the transformer may be adjusted after the test specimen has been brought to the desired temperature. The output signal obtained from the LVDT is proportional to the diameter change in the specimen.

---

* References are listed on Page

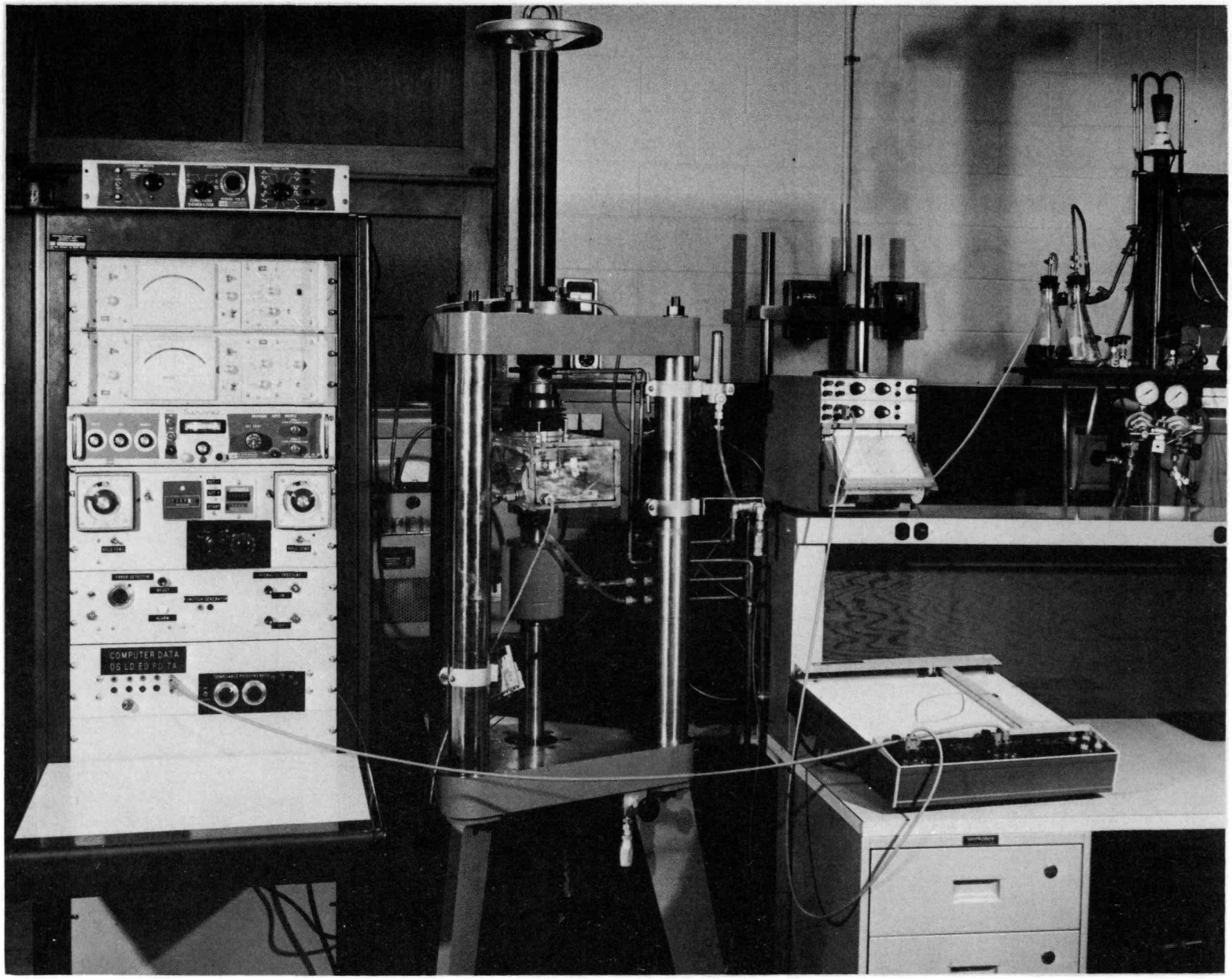

2754

FIGURE 7. CLOSED-LOOP ELECTROHYDRAULIC FATIGUE SYSTEM

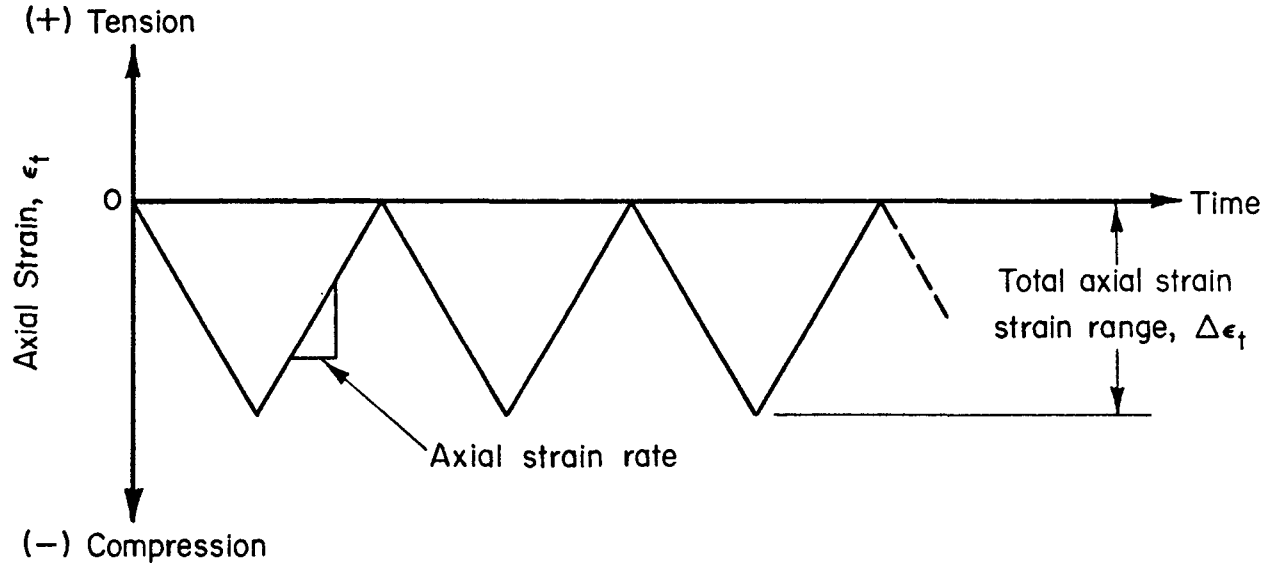

(a) Compression Strain–Cycling Waveform

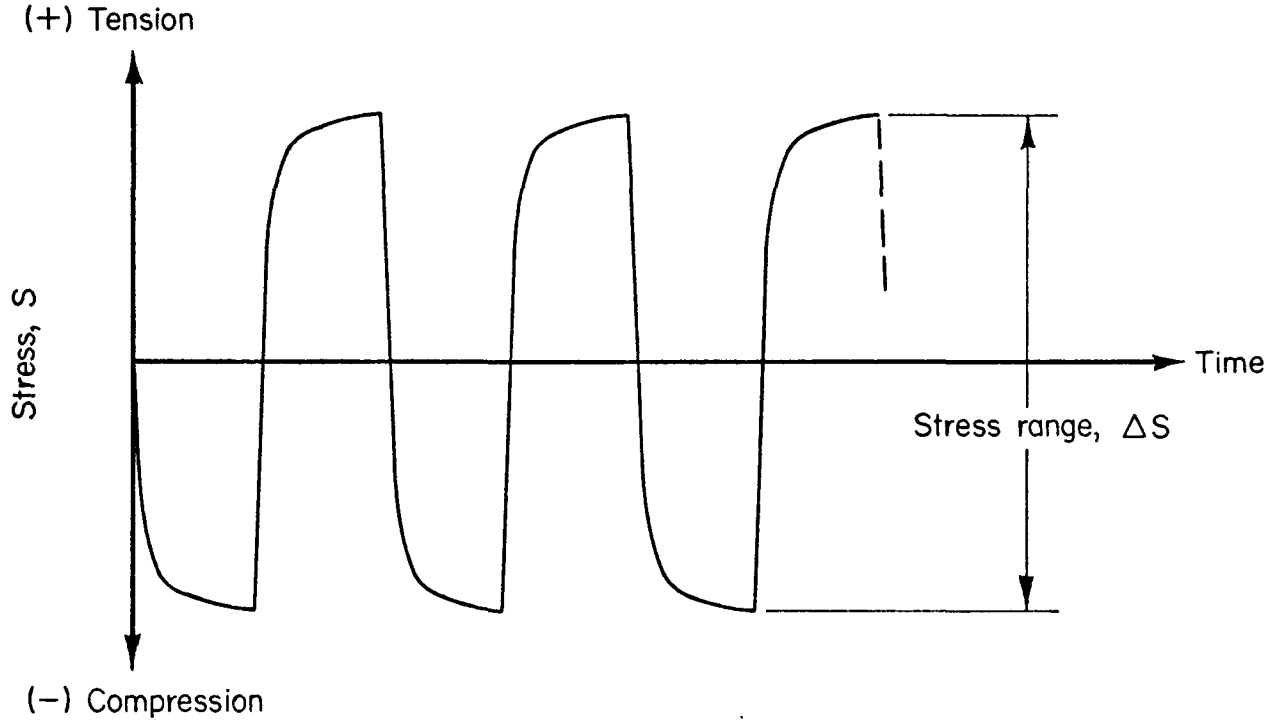

(b) Cyclic Stress Waveform

A-1112

FIGURE 8. CYCLIC WAVEFORMS OF AXIAL STRAIN AND STRESS

Specimens were heated by high-frequency induction, and temperature was controlled with a standard proprotional-type power controller. The geometry of the heating coil was designed to minimize temperature gradients in the test section. A specimen instrumented with several thermocouples along the central ½-inch portion was used to verify this design. Three Chromel-Alumel thermocouples were spot welded to the surface in the gage section of each specimen. Two of the thermocouples were 3/16 inch on one side of the minimum diameter. One of the first two thermocouples provided the feedback signal to the controller. The other two were used to make minor adjustments in the coil position and obtain a uniform temperature profile along the specimen.

Specimens were gripped using a fixture arrangement similar to that described by Feltner and Mitchell[2]. The lower end of the specimen was threaded tinto an adapter attached to the load cell which was, in turn, attached to the hydraulic actuator. The upper end of the specimen was attached to the loadframe crosshead through a Wood's metal type liquid-solid grip.[3] Both the upper and lower adapters were continuously water cooled to avoid overheating of the fixtures.

The high-purity hydrogen environment was obtained by a palladium alloy diffusion process. Commercial high-purity hydrogen (better than 99.95 percent) was supplied to a palladium catalyst purifier (Englehard Industries, Model HPD 20-150) that is capable of delivering 20 cubic feet per hour of ultrapure hydrogen. The hydrogen supplied to the test chamber by this system was virtually 100 percent pure (i.e., the extent to which contaminants are present in the gas is not measurable by any known means of detection). The test chamber (see Figure 9) was constructed of acrylic plastic sheet. It was sealed at the lower specimen grip by an "O" ring arrangement and sealed at the upper grip by a bellows. The chamber was large enough to encapsule the extensometer (see Figure 9). To insure a clean hydrogen atmosphere for the test, the chamber was first purged for 20 to 30 minutes with nitrogen. The high-purity hydrogen was then permitted to flow into the purged environment for approximately the same period of time before the induction heating of the specimen began. A flow of between 5 and 10 standard cubic feet per hour was maintained throughout the experiment; this amounts to roughly 8 to 16 volume changes of the hydrogen environment per hour. A pressure of at least 1 psig was maintained inside the chamber, and the gas which egressed from the chamber was burnt off at a remote point.

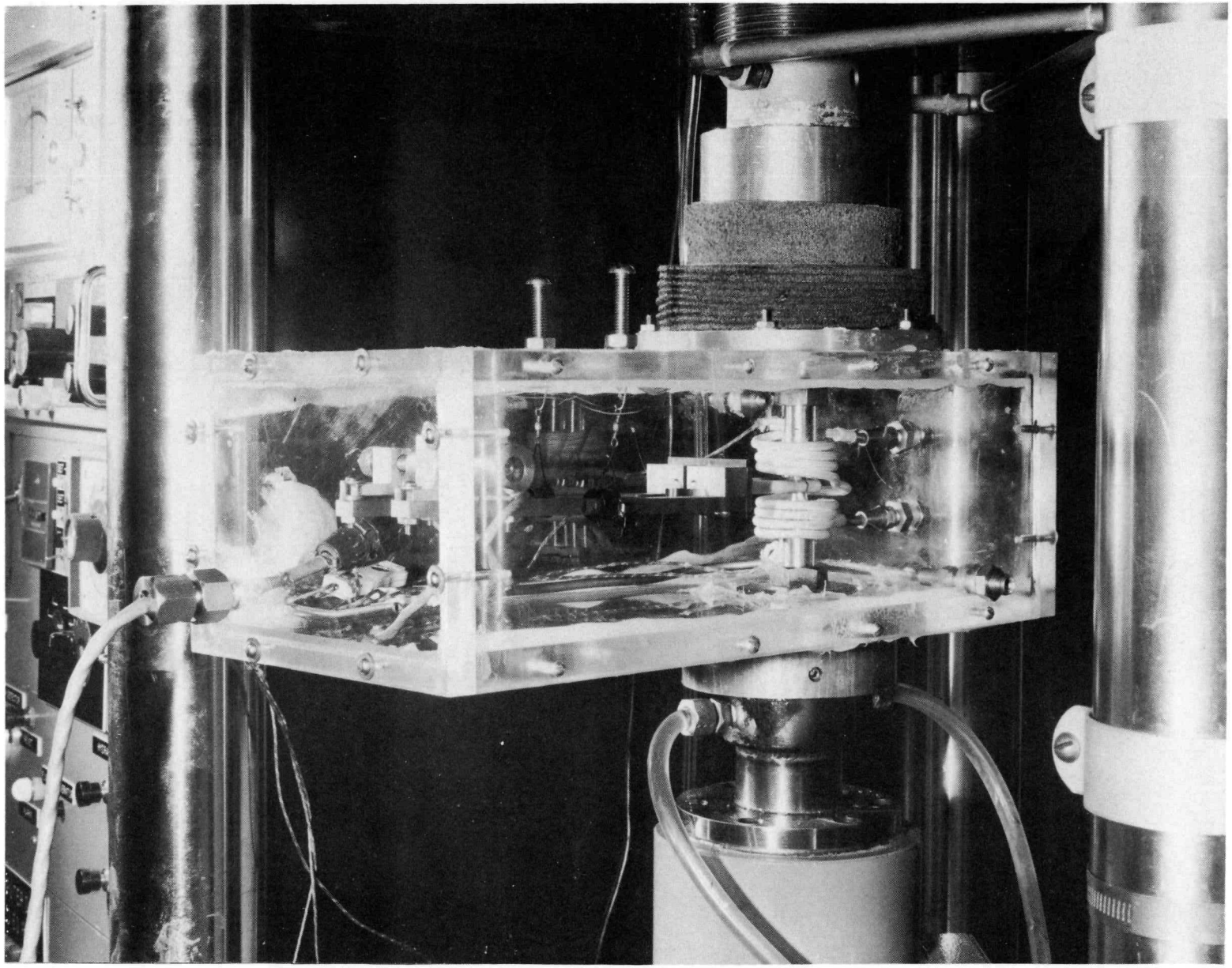

2812

FIGURE 9. HYDROGEN TEST CHAMBER WITH SPECIMEN INSTALLED

During each fatigue test, load was continuously recorded using a time-base strip chart recorder. These records were used to obtain hardening behavior and information on when cracking occurs just before total separation of the specimen. Load-axial extension hysteresis loops were periodically recorded during each test using an X-Y recorder. These loops were used to obtain values of total, plastic, and elastic strain range (see Figure 10 for definition of these terms).

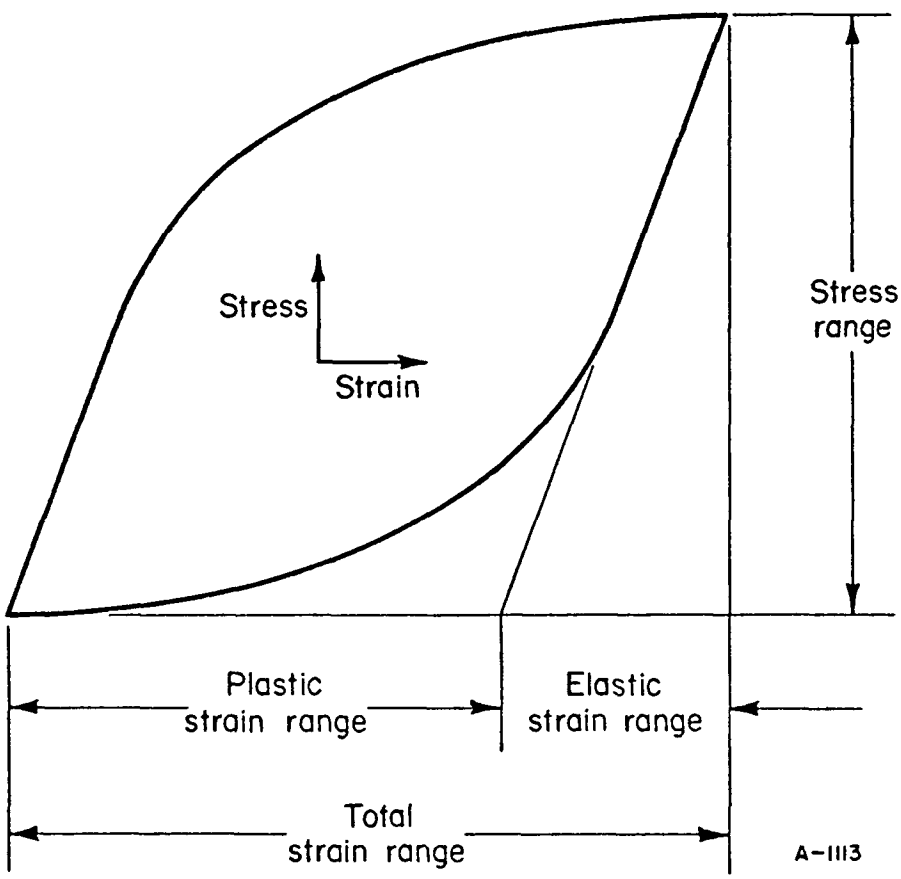

FIGURE 10. TERMS USED TO DEFINE HYSTERESIS LOOPS

Low-Cycle Fatigue Data Acquisition

Use of the hourglass-type specimen [see Figure 6(b)] in low-cycle fatigue evaluations of materials requires that the diametral, as opposed to axial, strain be measured. Because the axial strain is of prime interest, the diametral strain must be converted before the signal from the diametral extensometer can be effectively used in the control loop. To accomplish the conversion from diametral to axial strain, the elastic and plastic components of the diametral strain must be determined. Once these are found, the elastic and plastic components of axial strain can be computed and the results summed to generate the total axial strain. The necessary equations for the computation of axial strain and the analog circuits of the computer are described in detail by Slot, et al.[1] To practically complete the computations, the electric analogs of ϵ_d and P are supplied as inputs and the values of ν_e and K are fixed values programmed into the computer. The value of ν_p is generally taken as fixed at 0.5 assuming constant-volume plastic deformation of an isotropic material.

In this program, the value of Poisson's ratio for elastic deformation was calculated in the laboratory for each specimen. The specimen was installed in the test fixture, the hydrogen atmosphere was introduced, and the specimen was heated to the proper test temperature. The value of K was then set into the computer by load-cycling the specimen for several cycles at low loads in the elastic region and adjusting the K potentiometer until the value of ϵ_p was equal to zero. The value of Poisson's ratio was then determined from the equation

$$\nu_e = - \frac{\Delta\epsilon_{de} \, A_T E}{\Delta P} \quad , \tag{1}$$

where the values of $\Delta\epsilon_{de}$ and ΔP were determined from the slope of the load versus diametral extension X-Y plot recorded during a few load cycles after setting the value of K. A value for the modulus of elasticity was taken from data* described under the heading of "Discussion" in this report.

---

* Values of E used for the 1600 F tests were 19.5 x 10^3 ksi for Hastelloy X and 18.6 x 10^3 ksi for Type 347 stainless steel. These values were taken from the Materials Properties Data Book, Report 2275, Rev. of March 15, 1970, ANSC, Contract SNP-1.

Values of the cyclically stable strain (total, plastic, and elastic) range were obtained from the stable load versus axial extension hysteresis loops (see Figures 11 through 13) near half the fatigue life ($N_f/2$). Strain values were calculated by dividing the appropriate value of the extension by the gage length (minimum specimen diameter, D_T). Diameter was calculated at the temperature of the test. Figures 11 through 13 show representative hysteresis loops for the materials used in the program. The hysteresis loops shown for the beginning of the test illustrate the tendency of the material to harden due to cyclic straining. The other loops shown are typical of a stable hysteresis loop (or as near to stability as possible) for the corresponding conditions and material.

In addition to the recording of the load versus axial extension behavior, continuous cyclic load-time histories were recorded for every test. A representative cross section of the load histories during the early cycles are presented in Figures 14 through 16. These strip charts correspond to the displayed hysteresis loops described above. Examination of these charts reveals the materials' changing resistance to load as a function of strain cycles. The value of the stress at stability was determined from the load-time histories by reading the value of the load at $N_f/2$ and then dividing this value by the area of the specimen at the test temperature.

The load versus time histories were also used to determine the fatigue life of each specimen as defined by the following terms:

N_o = number of cycles where tension load started to drop off just before complete fracture occurred

N_5 = number of cycles were tension load dropped off 5 percent just before complete fracture occurred

N_f = number of cycles to complete fracture.

The value of N_o was difficult to determine experimentally and was only an approximate estimate of when cracking began. The value of N_5 was easier to determine and was a reasonably good definition of when a crack in the specimen had reached a significant size. The value of N_f was determined more exactly, but it probably was subject to more scatter than N_5, because the number of cycles from N_5 to N_f depends upon extensometer placement with

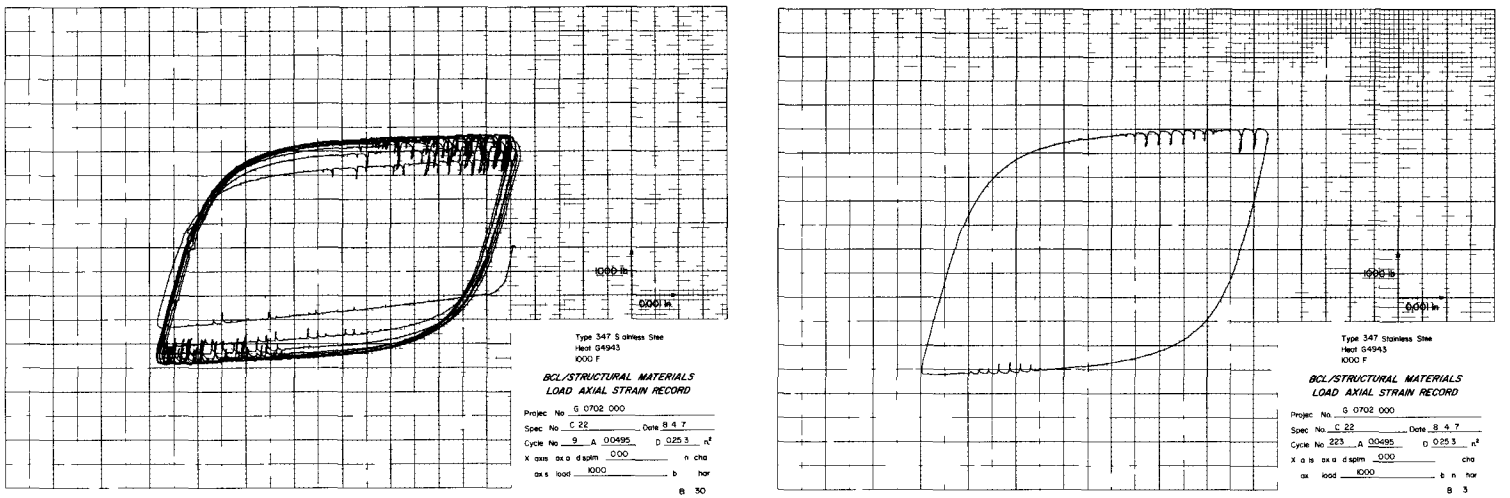

a. Type 347 Stainless Steel, $\Delta\varepsilon_t$ = 2.95 percent

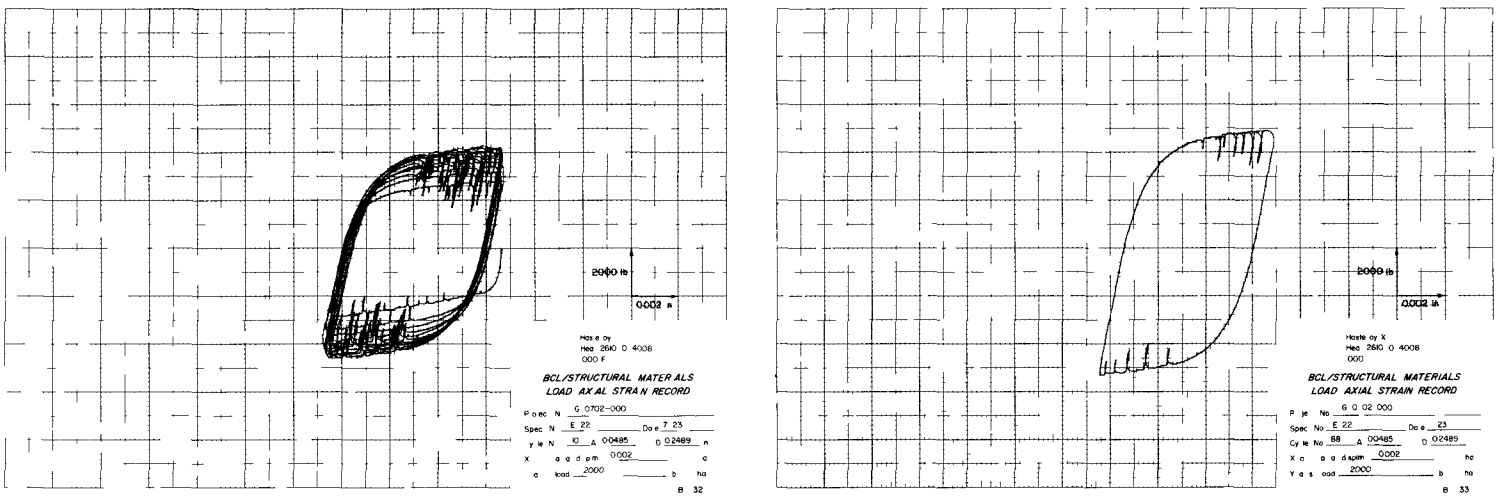

b. Hastelloy X, $\Delta\varepsilon_t$ = 2.95 percent

FIGURE 11. LOAD-AXIAL DISPLACEMENT HYSTERESIS LOOPS FOR TYPE 347 STAINLESS STEEL AND HASTELLOY X AT 1000 F

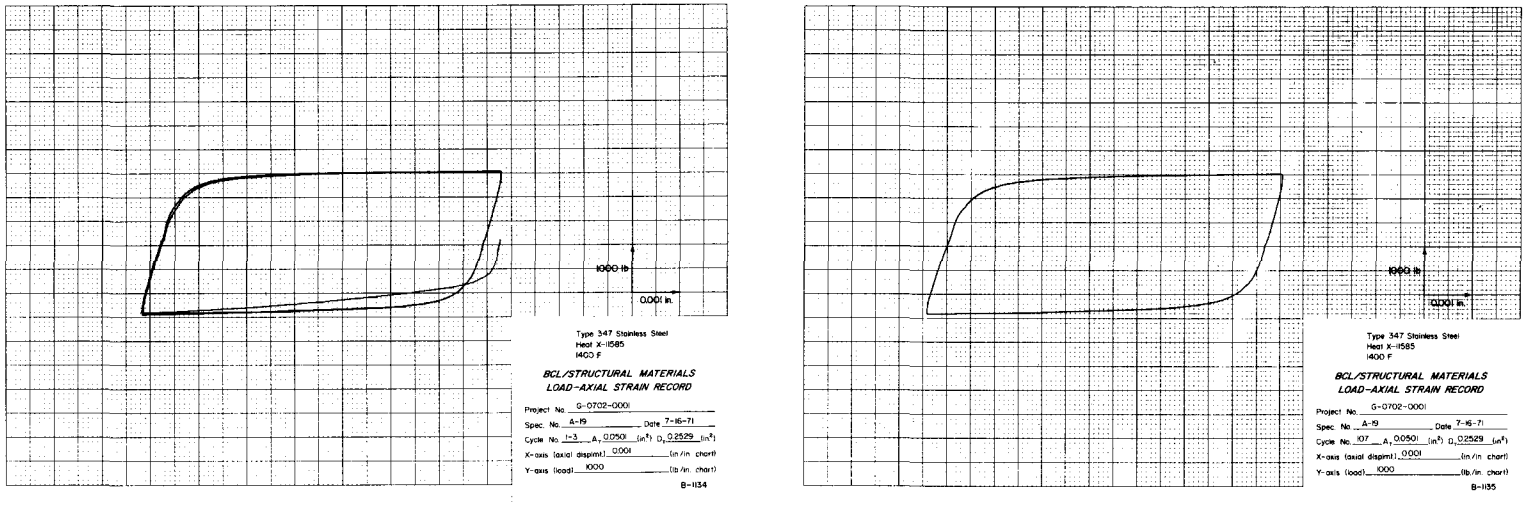

a. Type 347 Stainless Steel, $\Delta\varepsilon_t$ = 2.96 percent

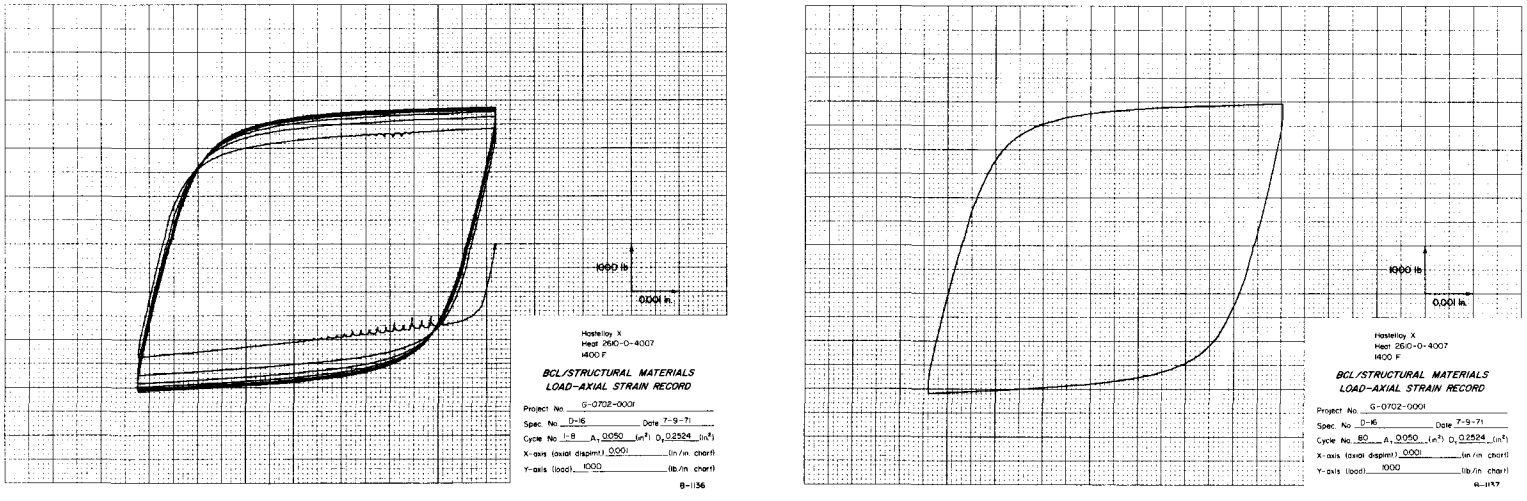

b. Hastelloy X, $\Delta\varepsilon_t$ = 2.96 percent

FIGURE 12. LOAD-AXIAL DISPLACEMENT HYSTERESIS LOOPS FOR TYPE 347 STAINLESS STEEL AND HASTELLOY X AT 1400 F

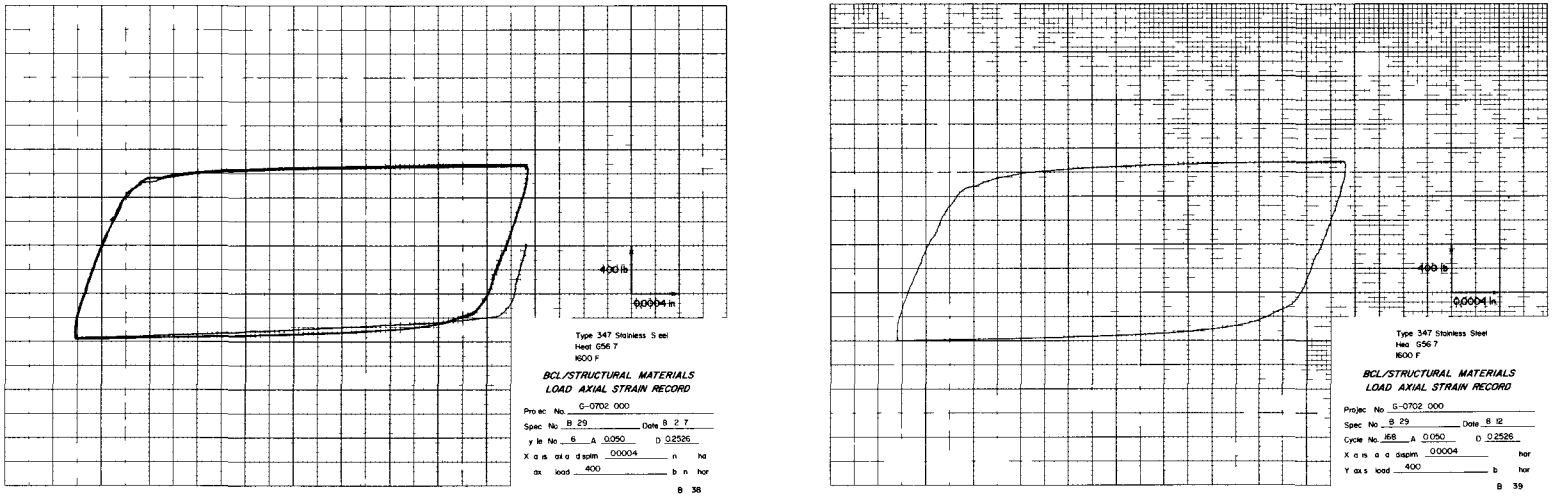

a. Type 347 Stainless Steel, $\Delta\varepsilon_t$ = 1.51 percent

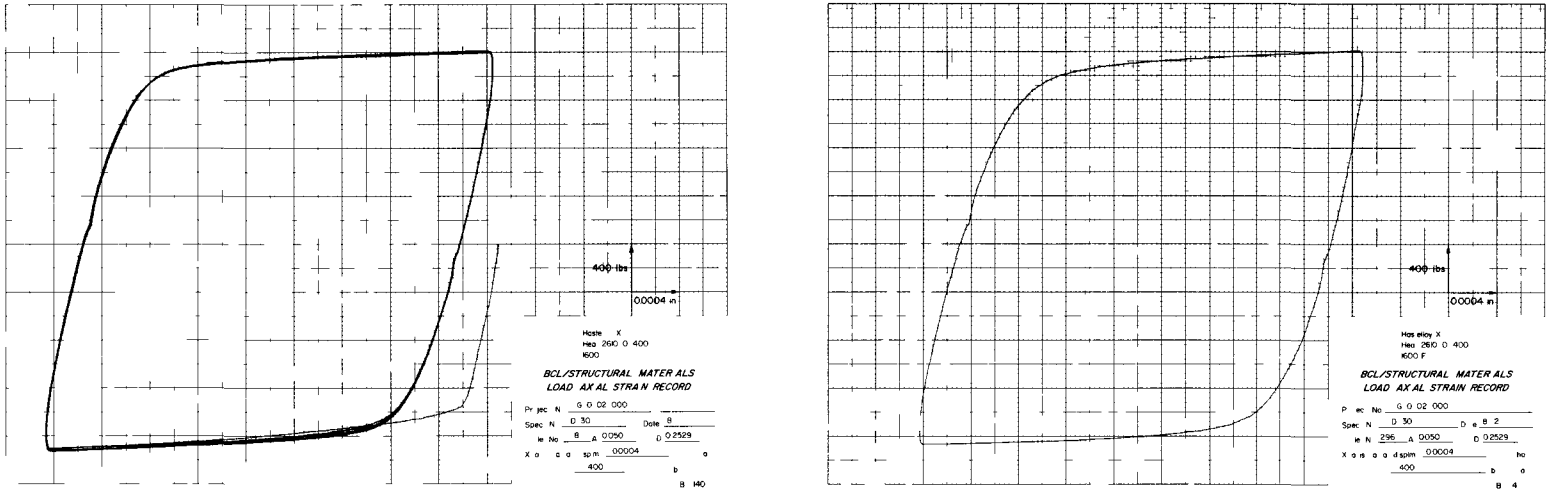

b. Hastelloy X, $\Delta\varepsilon_t$ = 1.91 percent

FIGURE 13. LOAD-AXIAL DISPLACEMENT HYSTERESIS LOOPS FOR TYPE 347 STAINLESS STEEL AND HASTELLOY X AT 1600 F

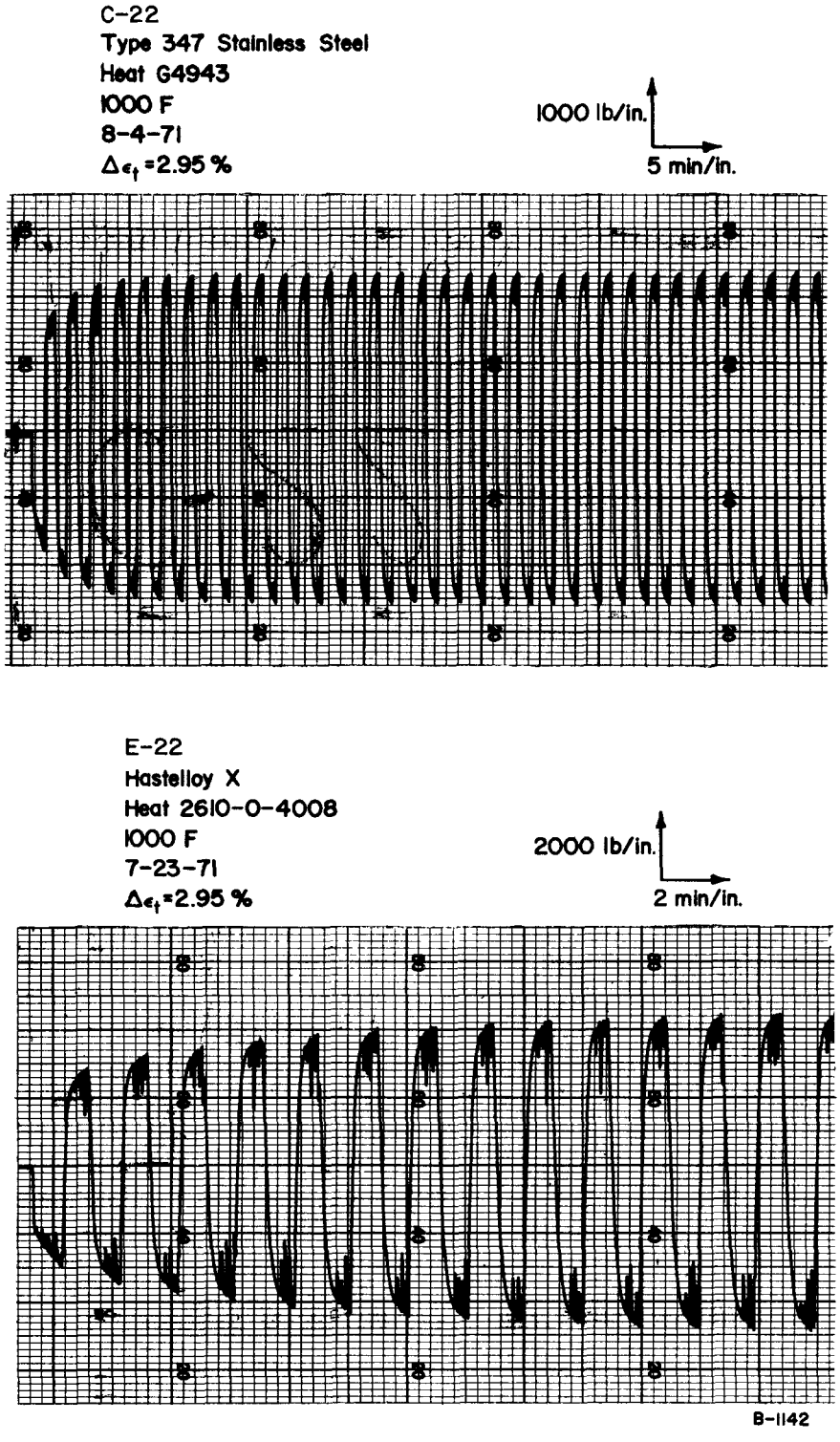

FIGURE 14. LOAD-TIME HISTORIES OF TYPE 347 STAINLESS STEEL AND HASTELLOY X AT 1000 F

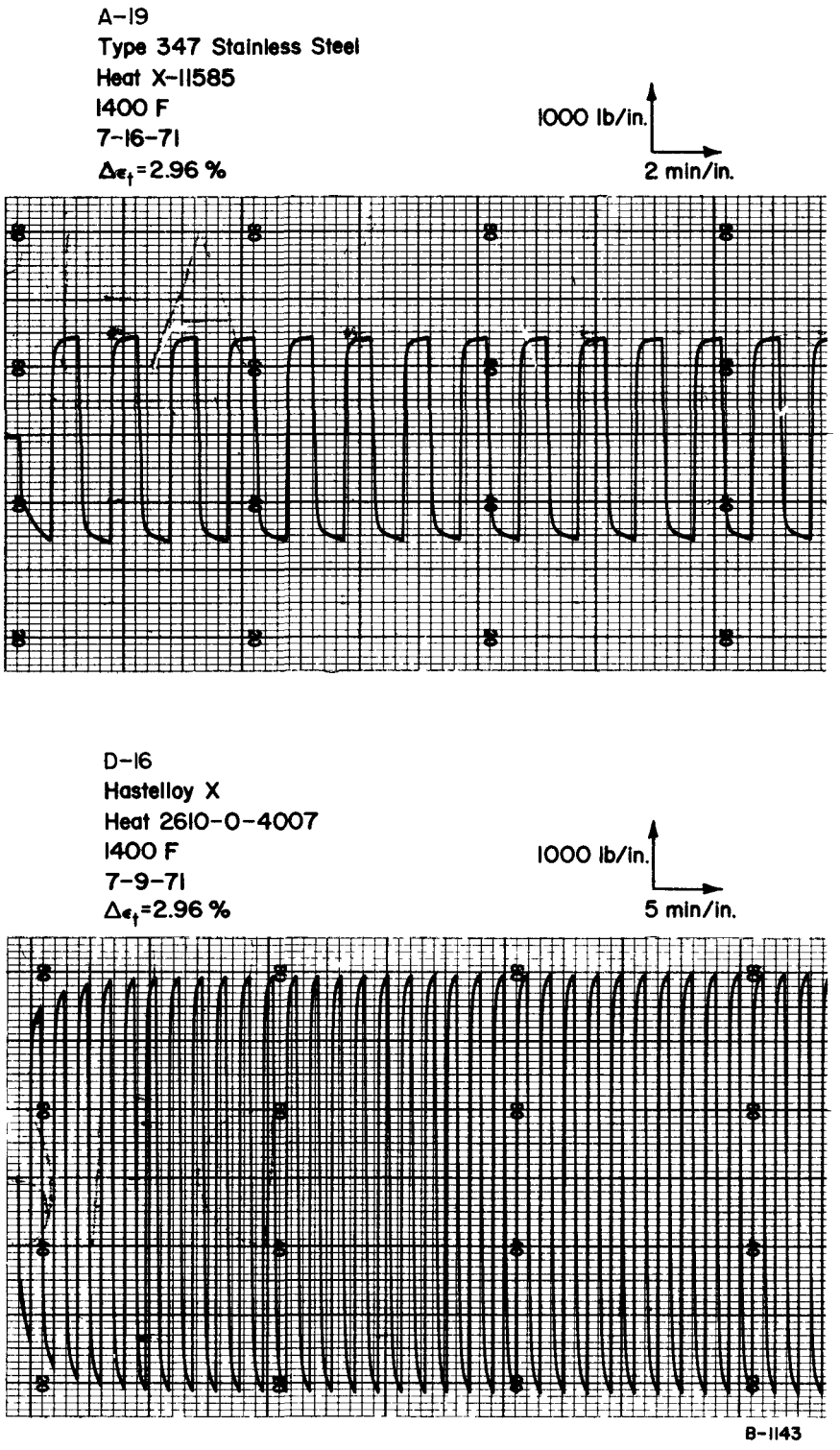

FIGURE 15. LOAD-TIME HISTORIES OF TYPE 347 STAINLESS STEEL AND HASTELLOY X AT 1400 F

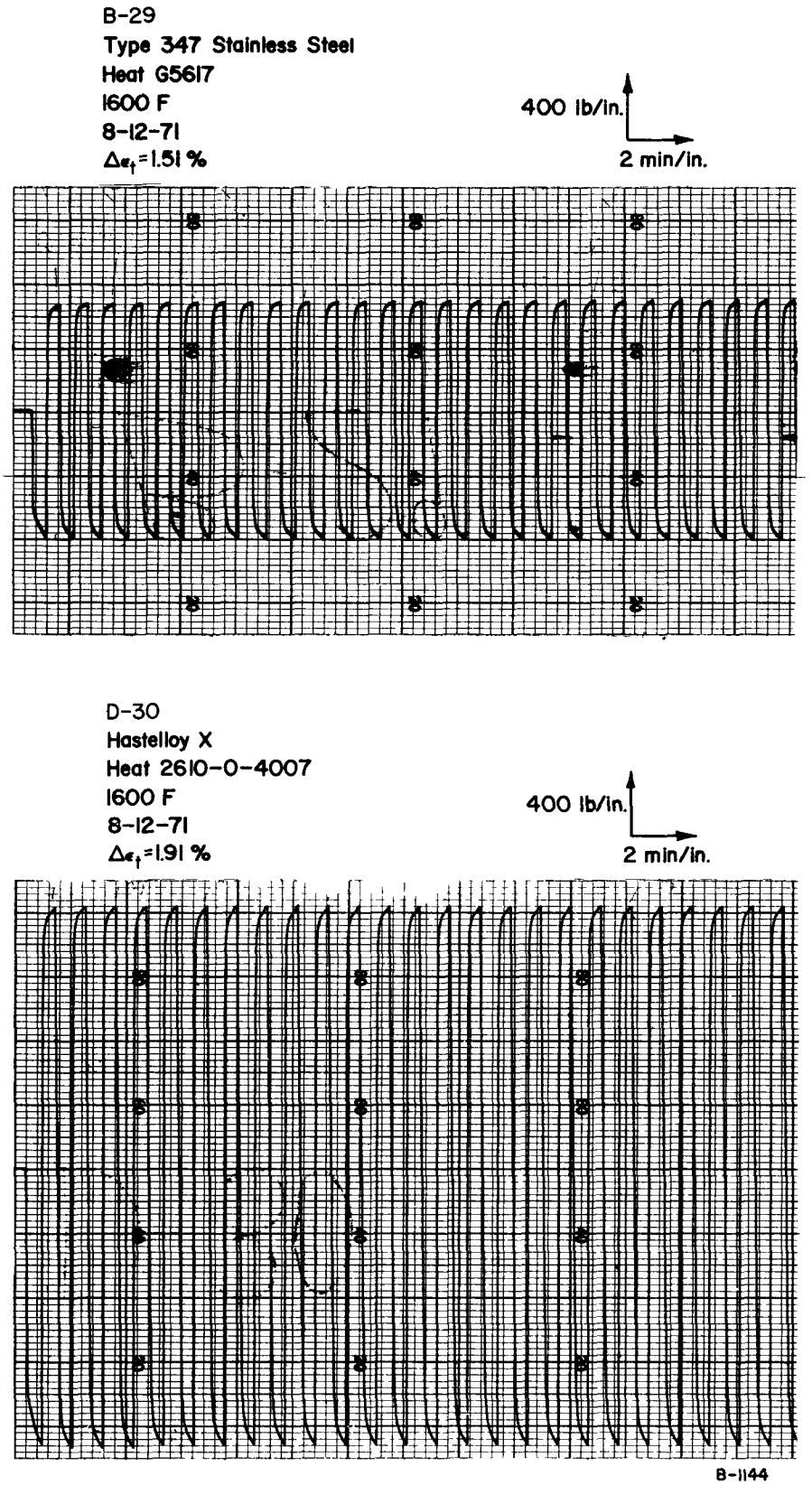

FIGURE 16. LOAD-TIME HISTORIES OF TYPE 347 STAINLESS STEEL AND HASTELLOY X AT 1600 F

respect to the exact location and orientation of the crack causing failure. In general, the ratio of N_s to N_f gives a qualitative indication of the resistance of the material to fatigue-crack propagation. Lower values of this ratio reflect higher resistance to crack propagation.

RESULTS AND DISCUSSION

Tensile

The room- and elevated-temperature tensile properties determined in this program are presented in Tables 2 and 3. Table 2 includes the data from the Type 347 stainless steel specimens, and Table 3 presents the data from the Hastelloy X tests. The tables are arranged to show the results of each test and an average value for all the tests at a given temperature. In general, the tensile ultimate strength and 0.2 percent offset yield strength values are slightly lower than normally expected for both Type 347 stainless steel and Hastelloy X. This trend may be related to the fact that the materials were subjected to a special heat-treatment cycle to simulate brazing operations. The influence of temperature on the above-mentioned strength properties is close to that usually seen for these alloys. The fracture ductility (as measured by percent elongation and percent reduction of area) of both alloys is close to the typical values at room temperature. At 1000 F, the ductility of Type 347 stainless steel (see Table 2) drops slightly below the value recorded for room temperature; at 1200 F, it is about the same as the value at room temperature; and at 1400 F, is a little higher than normal for this alloy. The Hastelloy X (see Table 3) has much higher than normal ductility at 1200 and 1400 F, while its ductility at 1000 F is similar to that at room temperature. This high fracture ductility is unusual for Hastelloy X because its ductility usually begins to decrease at 1000 F and reaches a minimum value, significantly lower than the room-temperature value, near 1400 F.

Stress-strain curves obtained from the tensile tests are presented in Figures 17 and 18. All curves, except those for Hastelloy X at 1000 F

TABLE 2. TENSILE PROPERTIES OF TYPE 347 STAINLESS STEEL AT A STRAIN RATE OF 0.005 MIN^{-1}

Temperature, F	Heat	Specimen	Modulus of Elasticity, ksi	0.2 Percent Offset Yield Strength, ksi	Ultimate Strength, ksi	Percent Elongation in 2 Inches	Percent Reduction of Area	True Fracture Ductility
RT	X-11585	AT1	24,700	32.5	88.3	54	71	1.24
	X-11585	AT2	25,500	31.3	87.0	53	71	1.22
	G5617	BT5	24,200	31.7	87.6	54	72	1.26
	G5617	BT6	24,900	31.3	88.2	56	72	1.26
	G4943	CT9	23,000	33.7	88.0	52	72	1.28
	G4943	CT10	22,800	33.3	88.0	52	72	1.27
	Average		24,200	32.3	87.8	53	72	1.25
1000	X-11585	AT13	21,500	19.5	57.0	36	64	1.03
	G5617	BT15	--	19.7	56.2	37	66	1.09
	G4943	CT17	24,600	20.1	55.5	36	65	1.05
	Average		23,000	19.8	56.2	36	65	1.06
1200	X-11585	AT14	22,800	18.8	45.0	46	72	1.26
	G5617	BT16	20,700	19.3	43.3	51	74	1.35
	G4943	CT18	25,000	19.1	43.7	49	72	1.27
	Average		22,800	19.1	44.0	49	73	1.29
1400	X-11585	AT3	22,500	16.3	28.9	59	82	1.69
	X-11585	AT4	19,800	16.7	28.6	58	81	1.64
	G5617	BT7	20,600	16.0	27.3	63	86	1.97
	G5617	BT8	17,200	15.9	27.1	64	86	1.93
	G4943	CT11	17,600	16.8	26.0	66	87	2.00
	G4943	CT12	18,800	16.7	26.3	66	87	2.00
	Average		19,400	16.4	27.4	63	85	1.87

TABLE 3. TENSILE PROPERTIES OF HASTELLOY X AT A STRAIN RATE OF 0.005 MIN^{-1}

Temperature, F	Heat	Specimen	Modulus of Elasticity, ksi	0.2 Percent Offset Yield Strength, ksi	Ultimate Strength, ksi	Percent Elongation in 2 Inches	Percent Reduction of Area	True Fracture Ductility
RT	2610-0-4007	DT1	26,300	51.7	115	42	52	0.73
	2610-0-4007	DT2	31,900	50.0	114	42	52	0.74
	2610-0-4008	ET5	28,900	50.6	115	42	52	0.73
	2610-0-4008	ET6	30,000	50.2	115	42	51	0.72
	Average		29,300	50.6	115	42	52	0.73
1000 F	2610-0-4007	DT9	26,300	37.8	96.5	42	51	0.71
	2610-0-4008	ET11	28,500	37.8	97.4	41	52	0.74
	Average		27,400	37.8	96.9	41	51	0.72
1200 F	2610-0-4007	DT10	23,600	37.3	83.5	59	72	1.27
	2610-0-4008	ET12	24,300	35.6	84.8	54	61	0.98
	Average		23,900	36.5	84.1	57	67	1.12
1400 F	2610-0-4007	DT3	20,400	32.8	52.9	84	86	1.97
	2610-0-4007	DT4	20,200	33.0	55.1	102	90	2.24
	2610-0-4008	ET7	22,200	32.5	57.0	82	75	1.37
	2610-0-4008	ET8	22,200	33.0	56.5	78	77	1.46
	Average		21,200	32.8	55.4	87	82	1.76

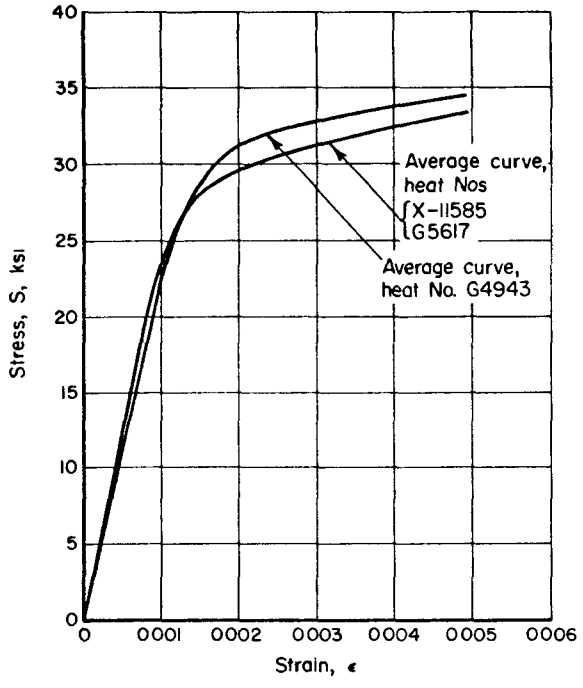

(a) Room Temperature (70 F)

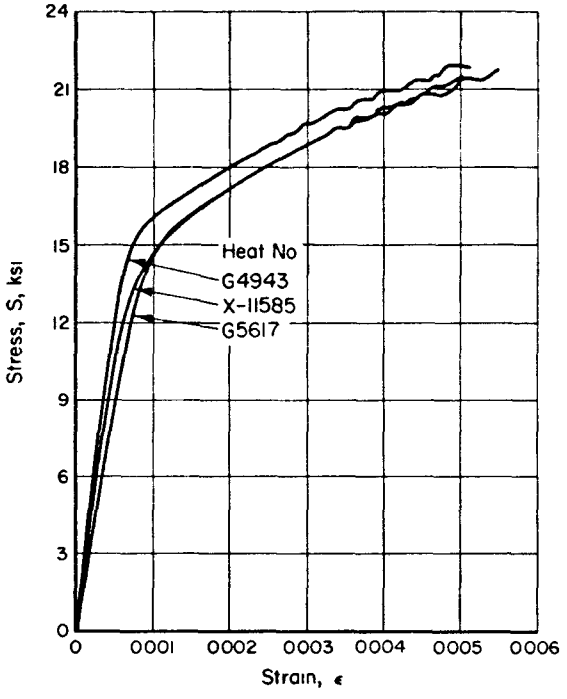

(b) 1000 F

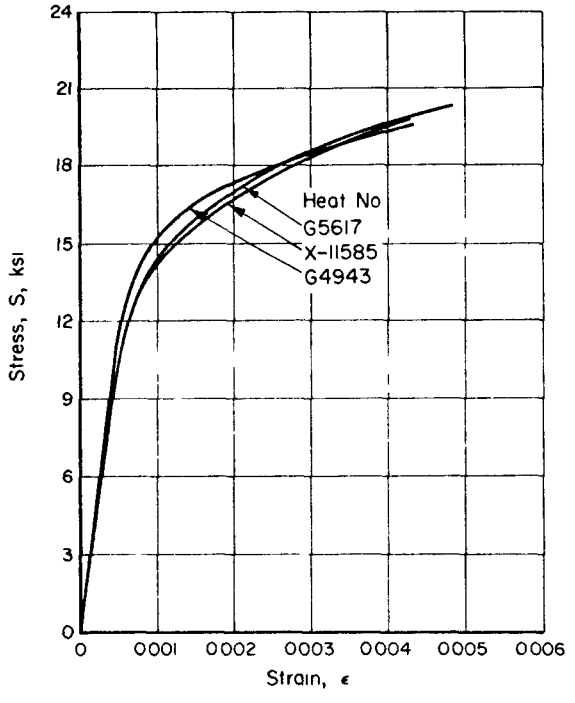

(c) 1200 F

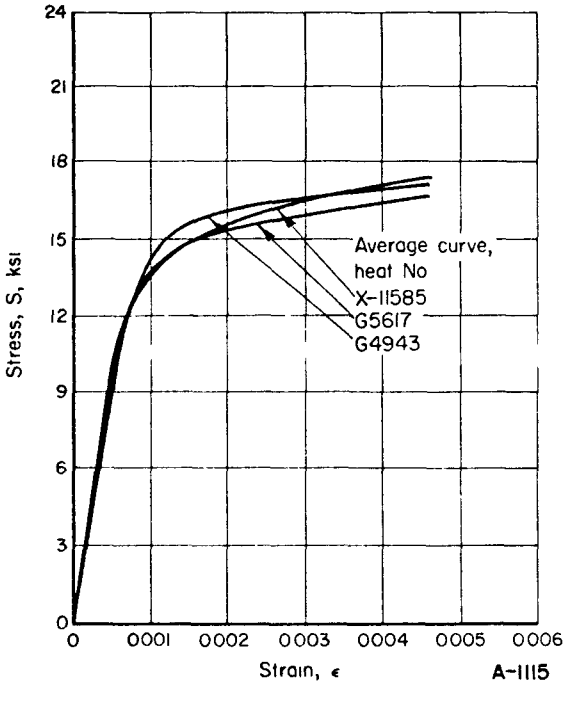

(d) 1400 F

FIGURE 17. MONOTONIC STRESS-STRAIN CURVES FOR TYPE 347 STAINLESS STEEL

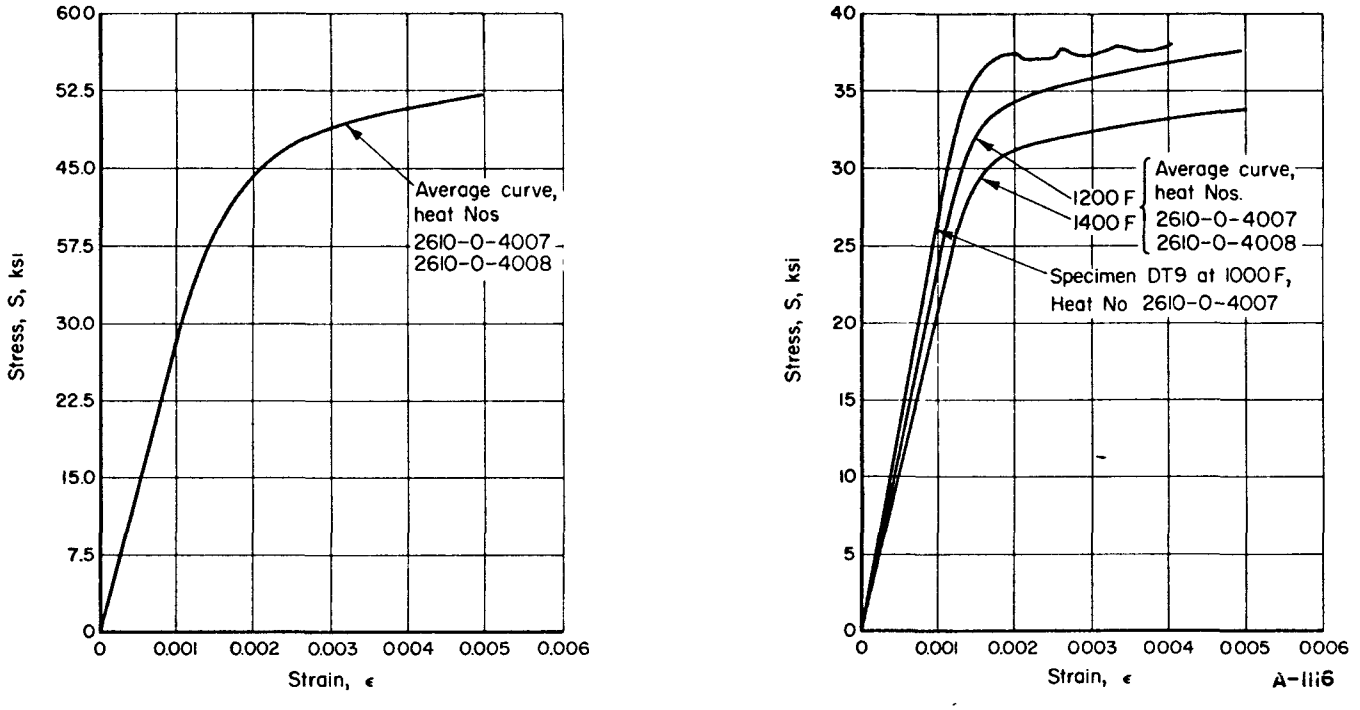

(a) Room Temperature (70 F)

(b) 1000, 1200, and 1400 F

FIGURE 18. MONOTONIC STRESS-STRAIN CURVES FOR HASTELLOY X

[see Figure 18(b)] and Type 347 stainless steel at 1000 and 1200 F [see Figures 17(b) and 17(c)], are average curves for the conditions indicated. The tensile stress-strain curves have been combined where duplicate tests of the same heat exhibited little variation. For Type 347 stainless steel at 1200 F, the curves [see Figure 17(c)] were not combined because at this temperature tensile tests were not duplicated within each heat. Both materials exhibited some instability in stress-strain response at 1000 F. This instability is defined as large decreases and increases in stress for small increases in strain in the plastic deformation regime of the material. The 1000 F curve for Hastelloy X [see Figure 18(b)] was from one specimen to show the abnormal type of stress-strain behavior exhibited at this temperature. Both specimens (DT9 and DT11) gave similar curves until yielding started to occur. Figure 17(b) shows this type of material instability for Type 347 stainless steel (the curves from all three of the specimens – AT13, BT15, and CT17 – are shown because it was believed they differed too much to be combined).

Low-Cycle Fatigue

Results of all low-cycle fatigue tests are summarized in Tables 4 through 12. With the exception of Table 4 which gives the results of several tests in air at 1400 F, all of the tables are arranged with the main emphasis on fatigue life. In each total strain range group (5.0 percent, 3.0 percent, and 1.5 percent) for each material, the data are tabulated in order of increasing fatigue life. This approach was taken in order to show any trends in fatigue life for the different heats of material. Originally, 51 tests in hydrogen gas environment were planned at each of the three test temperatures — 1000, 1400, and 1600 F. Actually, 53 tests were conducted at 1000 F, 52 tests were performed at 1400 F, and 67 specimens were tested at 1600 F.

The two additional specimens (D29 and E30) at 1000 F were to duplicate Specimens D20 and E23, respectively. The test on D20 was repeated because of its exceptionally long life which is believed to be the result of the low total strain range 1.21 percent) at which this test was run. Specimen E23 failed at the thermocouple welds after only 30 cycles. Because 30 cycles was well below the expected life, the test conditions were duplicated. Data from all 53 specimens tested at 1000 F are summarized in Tables 5 and 6. Examination of the fatigue life values in these tables shows no significant heat-to-heat variation for either material.

Results for the 52 specimens tested at 1400 F are reported in Tables 7 and 8. As at 1000 F, Type 347 stainless steel (Table 7) did not show a heat-to-heat variation in fatigue life. In contrast, Heat 2610-0-4008 (specimen prefix E) of Hastelloy X exhibited lower fatigue lives than Heat 2610-0-4007 (specimen prefix D) at 5.0 percent total strain range. (See Table 8.) However, this trend was not observed at the 3.0 percent strain range and was only slightly evident at the 1.5 percent strain range.

Tables 9 and 10 present the data obtained from 51 or the 67 specimens tested at 1600 F. The two heats of Hastelloy X did not exhibit any tendency toward a heat-to-heat variation in fatigue life. However, the Type 347 stainless steel had proclivity toward a heat-to-heat difference in fatigue life at the lowest strain range (1.5 percent). (See Table 9.) Specimens from Heat G5617 (with prefix B) had longer lives than specimens from both Heats G4943 (with prefix C) and X-11585 (with prefix A). Specimens from Heat G4943 displayed the shortest fatigue lives of the material at 1600 F.

TABLE 4. SUMMARY OF FATIGUE TESTS OF TYPE 347 STAINLESS STEEL AND HASTELLOY X IN AIR AT 1400 F AND AT AN AXIAL STRAIN RATE OF 10^{-3} SEC^{-1}

Specimen	Axial Strain Range at $N_f/2$, percent			Stress Range at $N_f/2$, ksi	Fatigue Life, cycles		
	Total	Plastic	Elastic		N_o	N_5	N_f
			Type 347 Stainless Steel				
A2[a]	1.57	1.29	0.28	62.5	430	465	655
A3	3.09	2.80	0.29	60.6	125	135	200
A4	5.10	4.73	0.37	66.8	60	78	96
A5	2.59	2.35	0.24	48.0	148	177	217
B1	5.11	4.77	0.34	70.6	80	87	118
B2	3.09	2.81	0.28	56.5	130	141	233
B3	3.31	2.99	0.32	61.0	140	157	219
B7	3.32	2.99	0.33	63.5	120	140	195
B8	1.64	1.34	0.30	54.5	300	330	485
B9	1.63	1.35	0.28	53.2	280	310	477
C1	2.64	2.42	0.22	51.1	137	167	197
C2	4.92	4.54	0.38	64.7	81	88	95
C4	1.64	1.32	0.29	51.5	400	420	591
			Hastelloy X				
D1	5.22	4.58	0.64	141	70	81	90
D2	3.18	2.65	0.53	124	145	157	184
D3	3.47	2.83	0.64	128	125	131	156
D4	1.66	1.14	0.52	105	420	441	540
E1	5.23	4.63	0.60	136	56	59	62
E2	3.22	2.62	0.60	124	116	118	128
E3	1.69	1.14	0.55	125	370	415	490
E5[a]	1.66	1.19	0.47	109	363	365	387

(a) Specimens A1 and E4 were lost in testing before any useful data could be obtained.

TABLE 5. FATIGUE TEST DATA FOR TYPE 347 STAINLESS STEEL, CONDUCTED IN A PURIFIED HYDROGEN ENVIRONMENT AT 1000 F AND AT AN AXIAL STRAIN RATE OF 10^{-3} SEC^{-1}

Specimen	Fatigue Life			Axial Strain Range at $N_f/2$, percent			Stress Range at $N_f/2$, ksi
	N_f, cycles	N_5, cycles	N_o, cycles	Total	Plastic	Elastic	
B24[a]	124	--	120	4.94	4.39	0.55	118.1
A21	132	125	121	4.92	4.38	0.54	121.5
B19[a]	142	--	141	4.94	4.34	0.60	122.3
B21	150	148	147	4.92	4.36	0.56	123.3
C15	155	153	153	4.93	4.40	0.53	122.0
C16	164	157	156	4.93	4.42	0.51	122.0
A25	170	167	166	4.97	4.41	0.56	120.7
A22	172	168	165	4.89	4.22	0.67	121.3
C17	174	172	171	4.92	4.25	0.67	122.0
A26	300	293	288	2.92	2.48	0.44	100.0
B26	327	320	307	2.91	2.37	0.54	109.0
C22	336	332	331	2.95	2.44	0.51	105.0
B25	339	337	336	2.92	2.43	0.49	107.0
C19	372	364	361	2.91	2.45	0.46	105.9
C21	397	373	367	2.92	2.46	0.46	106.5
A27[b]	401	--	--	2.92	2.38	0.54	112.5
A28	403	397	385	2.96	2.49	0.47	106.2
B27	405	389	382	2.89	2.44	0.45	105.5
C14	1369	1320	1303	1.50	1.13	0.37	86.8
B22	1590	1570	1555	1.48	1.11	0.37	88.5
A20	1856	1822	1812	1.49	1.10	0.39	88.0
B23	1877	1857	1840	1.38	1.01	0.37	84.5
C20	1952	1912	1810	1.49	1.08	0.41	86.7
A24	1975	1951	1949	1.48	1.07	0.41	84.5
A23	2251	2241	2238	1.46	1.04	0.42	86.2
C18	2443	2435	2425	1.47	1.12	0.35	81.2
B20	2536	2500	2495	1.39	0.99	0.40	82.0

(a) The values of N_o and N_5 are not defined for these because the load continued to increase until failure occurred.

(b) The value of N_5 is not reported because the tensile load did not drop off 5 percent before failure.

TABLE 6. FATIGUE TEST DATA FOR HASTELLOY X, CONDUCTED IN A PURIFIED HYDROGEN ENVIRONMENT AT 1000 F AND AN AXIAL STRAIN RATE OF 10^{-3} SEC^{-1}

Specimen	Fatigue Life			Axial Strain Range at $N_f/2$, percent			Stress Range at $N_f/2$, ksi
	N_f, cycles	N_5, cycles	N_o, cycles	Total	Plastic	Elastic	
E23	30	28	27	4.90	3.99	0.91	248.0
E19	51	49	48	4.85	3.70	1.15	242.5
D17	56	54	52	4.73	3.76	0.97	232.0
D28[a]	56	--	--	5.04	4.14	0.90	247.0
D25	81	79	76	5.02	4.16	0.86	235.0
D22	93	79	76	4.95	4.13	0.82	225.0
E20	98	96	93	4.75	3.65	1.10	232.5
E18	104	101	90	4.86	3.76	1.10	232.5
E30	104	94	92	4.96	4.12	0.84	230.0
D18	179	177	174	3.02	2.08	0.94	200.5
E22	194	176	171	2.95	2.22	0.73	214.0
D23[b]	212	--	210	3.01	2.28	0.73	206.3
E25	238	233	232	2.94	2.18	0.76	211.5
D27	240	238	233	2.96	2.18	0.78	214.0
E28	241	239	238	3.00	2.26	0.74	212.5
E29	289	288	287	2.96	2.17	0.79	215.0
D26	328	313	303	3.00	2.22	0.78	212.5
E21	846	830	820	1.49	0.88	0.61	168.5
D21	1029	1005	992	1.50	0.91	0.59	158.5
D24	1315	1313	1312	1.45	0.85	0.60	170.0
E27[c]	1589	--	--	1.50	0.92	0.58	164.5
E24	1644	1642	1642	1.50	0.93	0.57	162.5
D19	1775	1763	1756	1.26	0.67	0.59	144.2
E26	2193	2184	2183	1.40	0.83	0.57	155.0
D29	2205	2150	2143	1.46	0.90	0.56	153.0
D20	4750	4696	4694	1.21	0.58	0.63	147.0

(a) The values of N_o and N_5 are not defined for these tests because the load continued to increase until failure occurred.

(b) The value of N_5 is not reported because the tensile load did not drop off 5 percent before failure.

(c) The values of N_o and N_5 are not reported because the recorder malfunctioned before failure.

TABLE 7. FATIGUE TEST DATA FOR TYPE 347 STAINLESS STEEL, CONDUCTED IN A PURIFIED HYDROGEN ENVIRONMENT AT 1400 F AND AT AXIAL STRAIN RATE OF 10^{-3} SEC^{-1}

Specimen	Fatigue Life			Axial Strain Range at $N_f/2$, percent			Stress Range at $N_f/2$, ksi
	N_f, cycles	N_5, cycles	N_o, cycles	Total	Plastic	Elastic	
B11[a]	102	---	---	4.88	4.54	0.34	68.5
C6	111	105	104	4.92	4.56	0.36	65.5
A12	113	108	103	4.89	4.56	0.33	72.5
A11	119	113	111	4.88	4.54	0.34	68.6
C7	135	128	128	4.87	4.54	0.33	72.5
B10[b]	150	127	123	4.88	4.55	0.33	70.4
B12	162	155	150	4.87	4.53	0.34	68.5
A10[b]	168	160	160	4.89	4.52	0.37	76.4
C5[b]	191	185	182	4.85	4.53	0.32	65.5
B14[a]	162	---	---	2.94	2.64	0.30	65.5
A17	214	193	185	2.96	2.65	0.31	66.6
C9	238	227	222	2.95	2.60	0.35	66.5
B18	258	250	217	2.94	2.62	0.32	56.6
B15	260	246	243	2.95	2.59	0.36	63.6
A19	280	225	200	2.96	2.64	0.32	59.9
A13	286	260	235	2.94	2.62	0.32	64.5
C11	299	271	270	2.95	2.65	0.30	54.6
C10	368	327	325	2.95	2.64	0.31	57.5
B16[a]	648	---	---	1.49	1.19	0.30	52.2
A14	677	650	620	1.49	1.18	0.31	61.5
A16	691	683	682	1.49	1.24	0.25	54.8
A15	700	650	616	1.45	1.13	0.32	57.6
B13	739	520	515	1.49	1.24	0.25	53.3
B17	790	740	735	1.50	1.20	0.30	54.8
C13	796	760	760	1.46	1.17	0.29	50.4
A18	820	775	750	1.49	1.20	0.29	57.6
C8[a]	822	---	---	1.49	1.23	0.26	52.6
C12	950	879	850	1.50	1.23	0.27	54.5

(a) Values of N_o and N_5 are not reported because before failure occurred, the load began to increase.

(b) These specimens were tested in the "Nix Ox" catalyst purified hydrogen atmosphere; all others were tested in a palladium catalyst purified hydrogen atmosphere.

TABLE 8. FATIGUE TEST DATA FOR HASTELLOY X, CONDUCTED IN A PURIFIED HYDROGEN ENVIRONMENT AT 1400 F AND AN AXIAL STRAIN RATE OF 10^{-3} SEC^{-1}

Specimen Number	Fatigue Life			Axial Strain Range at N_f, percent			Stress Range at $N_f/2$, ksi
	N_f, Cycles	N_5, Cycles	N_o, Cycles	Total	Plastic	Elastic	
E8 (a)	50	49	49	4.91	4.28	0.63	146
E6 (a)	59	58	57	4.89	4.23	0.66	144.4
E13(b)	61	--	53	4.92	4.36	0.56	137.5
E7 (a)	67	64	64	4.92	4.33	0.59	144.6
D14	99	97	80	4.92	4.29	0.63	129.5
D5 (a)	108	106	105	4.88	4.31	0.57	145.4
D7 (a)	136	134	132	4.93	4.34	0.59	134.5
D6 (a)	137	134	134	4.88	4.25	0.63	144
D16(b)	203	---	201	2.96	2.41	0.55	124
E16	228	227	223	2.92	2.32	0.60	119.2
D15	230	228	227	2.96	2.39	0.57	122.5
D10	251	235	232	2.98	2.32	0.66	119
E10	262	250	247	2.84	2.24	0.60	114.7
E17	275	265	255	2.92	2.30	0.62	113.5
D9	283	252	251	2.94	2.44	0.50	118
E11	314	255	230	2.93	2.38	0.55	107
E9	629	577	573	1.45	0.99	0.46	108.5
E14(c)	708	---	---	1.48	1.04	0.44	105.5
E12	720	685	675	1.47	1.03	0.44	109
D11	865	833	825	1.47	0.99	0.48	104.7
D8	923	880	875	1.50	1.03	0.47	108.3
D12	929	915	912	1.47	0.99	0.48	106.7
E15	935	860	840	1.44	0.94	0.50	97.5
D13	964	895	880	1.47	0.97	0.50	96.7

(a) These specimens were tested in a "Nix Ox" cayalyst purified hydrogen atmosphere; all others were tested in a palladium catalyst purified hydrogen atmosphere.

(b) The value of N_5 is not reported because the tensile load did not drop off 5 percent before failure occurred.

(c) Values of N_o and N_5 are not reported because before failure occurred, the load began to increase.

TABLE 9. FATIGUE TEST DATA FOR TYPE 347 STAINLESS STEEL, CONDUCTED IN A PURIFIED HYDROGEN ENVIRONMENT AT 1600 F AND AT AN AXIAL STRAIN RATE OF 10^{-3} SEC^{-1}

Specimen	Fatigue Life N_f, cycles	Fatigue Life N_5, cycles	Fatigue Life N_o, cycles	Axial Strain Range at $N_f/2$, percent: Total	Axial Strain Range at $N_f/2$, percent: Plastic	Axial Strain Range at $N_f/2$, percent: Elastic	Stress Range at $N_f/2$, ksi
C34	139	--	--	5.12	4.96	0.16	29.2[a]
B37	151	140	90	4.96	4.78	0.18	31.9
A37	178	171	82	4.93	4.74	0.19	33.9
C26	190	165	80	5.32	5.15	0.17	29.6
A36	241	200	120	4.97	4.80	0.17	33.3
B36	294	260	210	5.30	5.14	0.16	28.7
A29	356	352	100	4.97	4.77	0.20	30.1
B30[b]	359	210	150	4.96	4.80	0.16	25.9
C35	482	315	220	4.95	4.81	0.14	26.3
B35	232	--	--	3.00	2.81	0.19	35.2[a]
A38	437	410	255	3.20	3.02	0.18	30.3
A39	446	430	250	2.96	2.78	0.18	29.6
B31	479	445	320	2.97	2.81	0.16	25.7
C30	479	--	--	2.94	2.77	0.17	31.2[a]
C31	516	--	--	2.94	2.77	0.17	31.8[a]
B34	517	--	--	2.95	2.80	0.15	28.4[a]
C29	553	--	--	2.94	2.77	0.17	27.6[a]
A32	754	520	450	2.98	2.81	0.17	27.4
C32	767	700	500	1.70	1.55	0.15	30.3
C25[b]	1522	1430	800	1.50	1.33	0.17	29.2
A35	1821	1805	850	1.47	1.32	0.15	27.6
C33	1889	1550	900	1.48	1.32	0.16	29.5
C28	1913	--	--	1.45	1.31	0.14	26.5[a]
A33	2000	1720	1000	1.44	1.33	0.11	23.0
A31	2111	1850	1750	1.28	1.12	0.16	27.1
B38	2124	1650	800	1.50	1.35	0.15	28.4
B32	2245	1600	1200	1.48	1.33	0.15	29.7
B39	2545	2200	2100	1.44	1.30	0.14	26.1
B40	2850	1750	1400	1.48	1.32	0.16	29.1

(a) Values of N_o and N_5 are not reported because anomolies in the load versus cycles record make their determination ambiguous.

(b) Hydrogen gas was purified using a copper chip drier and the specimen surface was similar to that obtained using a palladium-catalyst purifier.

TABLE 10. FATIGUE TEST DATA FOR HASTELLOY X, CONDUCTED IN A PURIFIED HYDROGEN ENVIRONMENT AT 1600 F AND AN AXIAL STRAIN RATE OF 10^{-3} SEC^{-1}

Specimen	Fatigue Life			Axial Strain Range at $N_f/2$, percent			Stress Range at $N_f/2$, ksi
	N_f, cycles	N_5, cycles	N_o, cycles	Total	Plastic	Elastic	
E39	172	155	88	5.27	4.96	0.31	66.9
D44	185	170	80	5.19	4.84	0.35	61.0
E34	185	182	90	5.01	4.67	0.34	67.6
D41	193	--	--	5.01	4.66	0.35	68.5[a]
E35	194	182	95	4.97	4.68	0.29	63.0
E38	219	192	100	4.96	4.65	0.31	63.5
D45	255	170	115	4.95	4.64	0.31	63.9
D40	277	268	150	4.96	4.62	0.34	59.6
E42	301	265	120	3.34	3.01	0.33	57.8
E40	425	--	--	3.00	2.70	0.30	65.0[a]
D36	469	440	185	3.00	2.67	0.33	65.1
D39	473	--	--	3.00	2.67	0.33	64.0[a]
E36	479	465	300	3.00	2.68	0.32	63.0
D37	522	--	--	2.95	2.62	0.33	62.5[a]
E33	596	582	290	2.96	2.59	0.37	60.1
D47	621	520	350	2.96	2.65	0.31	63.8
E41	981	900	450	1.65	1.33	0.32	64.8
D43	1601	--	--	1.49	1.20	0.29	57.4[a]
D35[b]	1731	1660	1000	1.53	1.19	0.34	60.0
D42	1805	1650	700	1.59	1.27	0.32	63.1
E31[c]	1896	--	--	1.52	1.25	0.27	62.1[a]
E37	1998	1825	960	1.53	1.23	0.30	56.3
D46	2249	2000	950	1.51	1.22	0.29	64.4
E32	2278	1950	1000	1.51	1.22	0.29	58.4
D38	2283	--	--	1.48	1.18	0.30	56.8

(a) Values of N_o and N_5 are not reported because anomolies in the load versus cycles record make their determination ambiguous.

(b) Hydrogen gas was purified using a copper chip drier and the specimen surface was similar to that obtained using a palladium-catalyst purifier.

(c) Specimen was covered with green oxide in test section because of a malfunction in the hydrogen gas purification system.

TABLE 11. DUPLICATED SPECIMENS

Specimens Duplicated Due to the Formation of a Green Oxide During the Test

Original Specimen	Duplicate Specimen	Fatigue Life N_f, cycles	Fatigue Life N_5, cycles	Fatigue Life N_o, cycles	Axial Strain Range at $N_f/2$, percent Total	Axial Strain Range at $N_f/2$, percent Plastic	Axial Strain Range at $N_f/2$, percent Elastic	Stress Range at $N_f/2$, ksi
C24	C35	119	110	70	6.64	6.46	0.18	32.1
B33	B37	134	105	80	5.24	5.07	0.17	30.1
A34	A37	137	97	70	5.23	5.10	0.13	24.7
C23	C34	206	165	100	6.64	6.47	0.17	31.7
A30	A39	347	225	170	3.00	2.81	0.19	31.1
B29	B40	929	785	782	1.51	1.36	0.15	30.4
B28	B39	982	960	450	1.49	1.30	0.19	28.8
C27	C33	1135	--	--	1.65	1.49	0.16	27.7[(a)]

(a) Values of N_o and N_5 are not reported because anomolies in the load versus cycles record make their determination ambiguous.

TABLE 12. DUPLICATED SPECIMENS

Specimens Duplicated Due to Their Abnormally High Strain Ranges

Original Specimen	Duplicate Specimen	Fatigue Life N_f, cycles	Fatigue Life N_5, cycles	Fatigue Life N_o, cycles	Axial Strain Range at $N_f/2$, percent: Total	Axial Strain Range at $N_f/2$, percent: Plastic	Axial Strain Range at $N_f/2$, percent: Elastic	Stress Range at $N_f/2$, ksi
D31[a]	D44	103	--	--	6.66	6.28	0.38	68.0[c]
D32[b]	D45	129	97	47	6.64	6.24	0.40	69.5
D33[b]	D47	227	204	122	3.95	3.57	0.38	74.8
D34[b]	D46	784	700	400	1.96	1.63	0.33	71.9
D30[a]	D43	808	730	350	1.91	1.57	0.34	66.3

(a) Specimen was covered with green oxide in test section because of a malfunction in the hydrogen gas purification system.

(b) Hydrogen gas was purified using a copper chip drier and the specimen surface was similar to that obtained using a palladium-catalyst purifier.

(c) Values of N_o and N_5 are not reported because anomolies in the load versus cycles record make their determination ambiguous.

Tables 11 and 12 report the results at 1600 F that were at abnormal conditions with regard to the original test matrix. The number of the duplicate specimen that replaced each of these in the test matrix is included for reference purposes. Listed in Table 11 are data for eight specimens of Type 347 stainless steel where improper hydrogen purification caused the formation of a green oxide on the test surface. Because these specimens had shorter fatigue lives than specimens tested in the nominal hydrogen environment, the results were not included in subsequent data analyses. As reported in Table 12, five specimens of Hastelloy X were unintentionally tested at higher than desired strain ranges. Since these latter results were still valid, they were included in subsequent data analyses.

Figures 19 through 21 are plots of stress amplitude versus fatigue life that show representative cyclic hardening or softening characteristics of the materials for the conditions indicated. Figures 19(a) and 19(b) show the characteristic cyclic hardening behavior of Type 347 stainless steel and Hastelloy X, respectively, at 1000 F. At this temperature, both materials hardened regardless of strain range; however, Hastelloy X hardened considerably more than Type 347 stainless steel. At 1400 F (see Figures 20(a) and 20(b), the stainless steel showed only a slight tendency to cyclically harden, while Hastelloy X still cyclically hardened. It is seen in Figure 20(a) that Hastelloy X hardened very rapidly at the 5.0 percent axial strain range as compared to its gradual hardening at the 1.5 percent strain range. Figures 21(a) and 21(b) show that the materials did not cyclically harden at 1600 F. The Type 347 stainless steel [Figure 21(a)] had a relatively constant stress amplitude at the 1.5 and 3.0 percent strain ranges; however, at 5.0 percent axial strain, the material cyclically softened. Hastelloy X had a relatively constant stress amplitude at all three strain ranges as illustrated in Figure 21(b).

The remaining figures illustrate the low-cycle fatigue resistance of the materials. Figures 22 through 24 are arranged to show the characteristics of each individual heat at each test temperature. These figures are plots of strain range (total, plastic, and elastic) versus fatigue life. Figures 25(a) (b), and (c) are composites of only the total strain range versus fatigue life curves from the first five figures. The elastic strain range and plastic strain range curves were not treated in this manner because the total strain

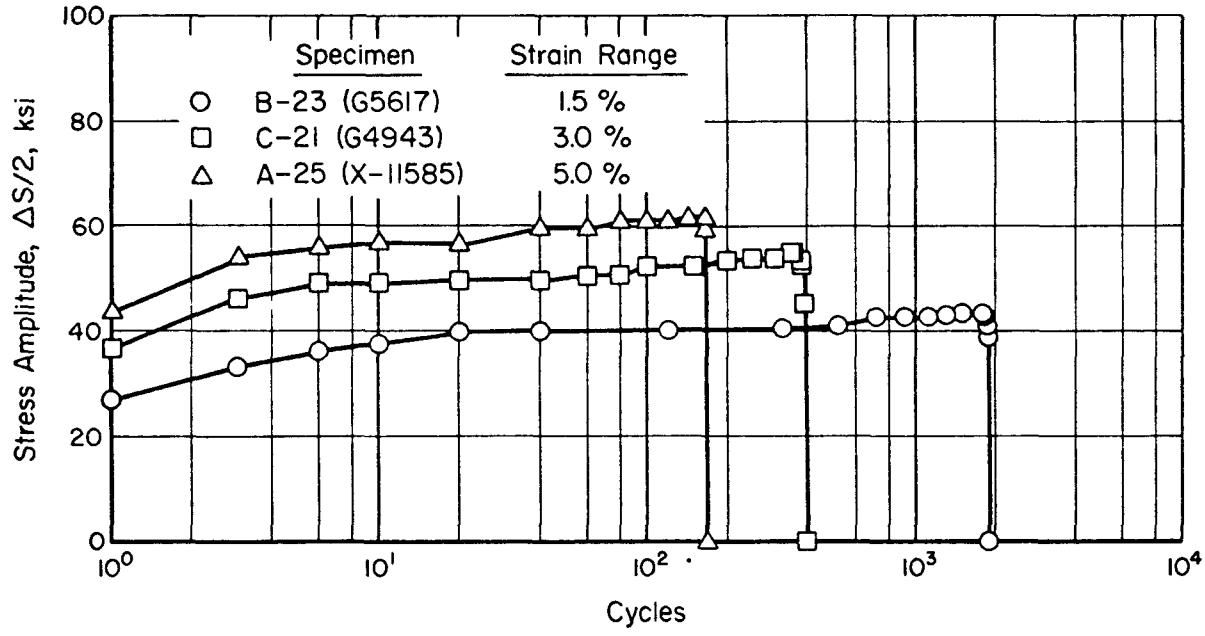

a. Type 347 Stainless Steel

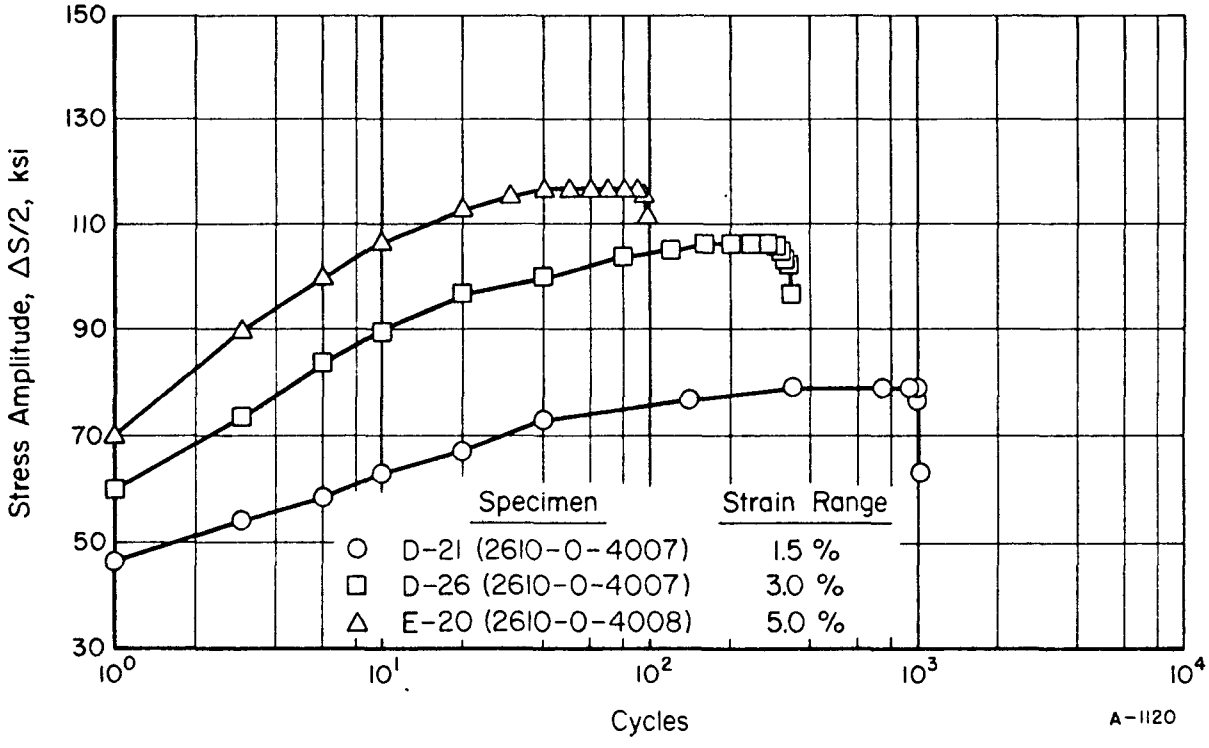

b. Hastelloy X

FIGURE 19. STRESS AMPLITUDE, ΔS/2, VERSUS FATIGUE LIFE, N_f, FOR TYPE 347 STAINLESS STEEL AND HASTELLOY X AT 1000 F

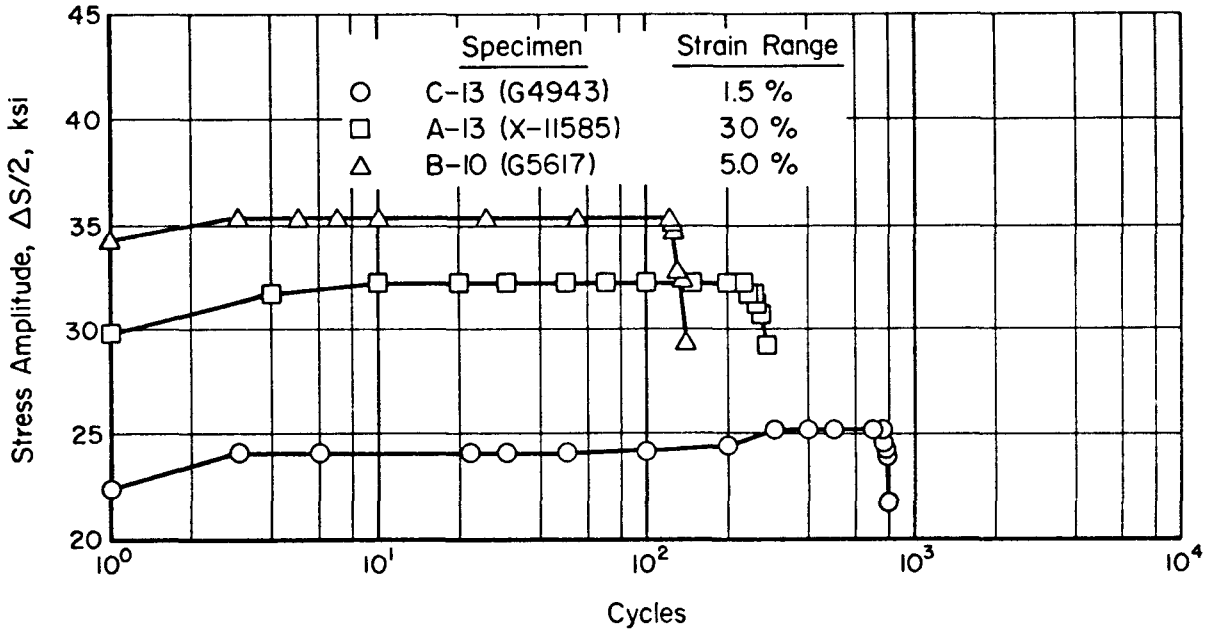

a. Type 347 Stainless Steel

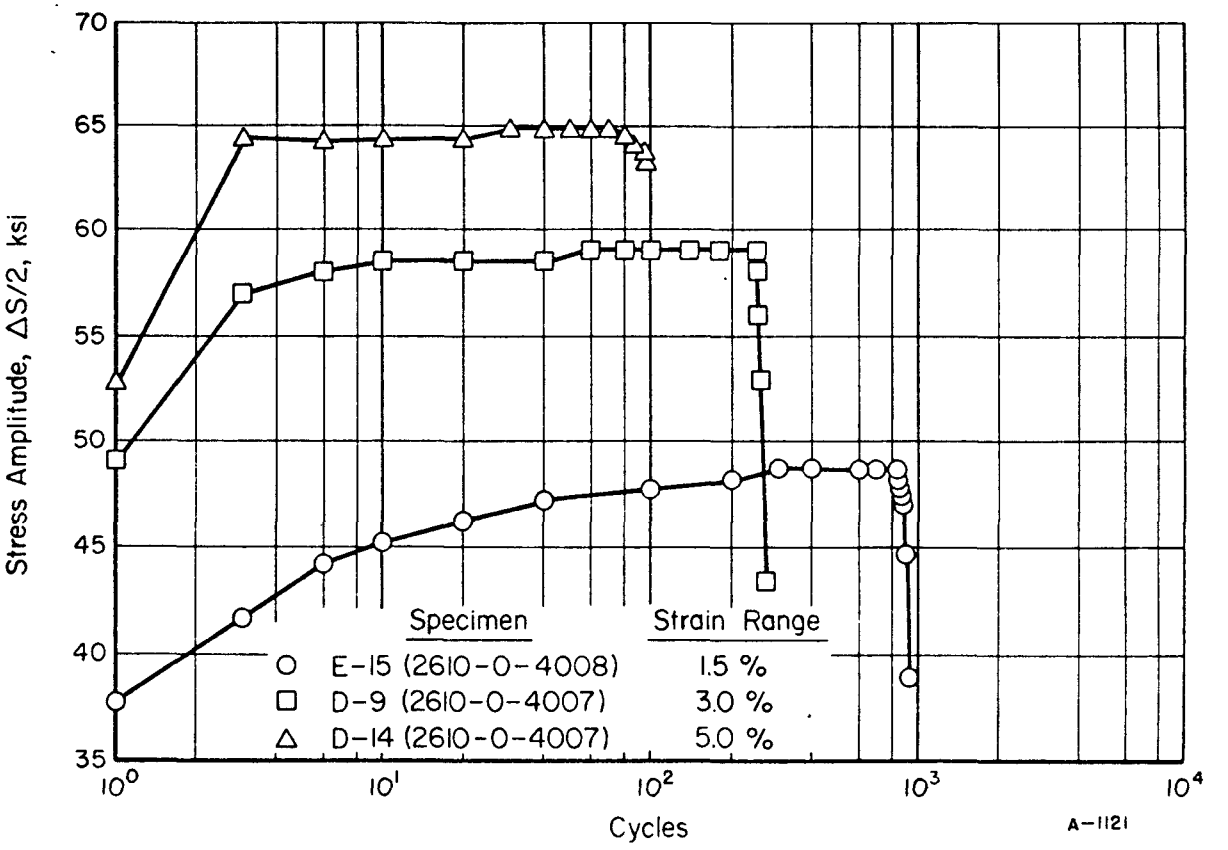

b. Hastelloy X

FIGURE 20. STRESS AMPLITUDE, ΔS/2, VERSUS FATIGUE LIFE, N_f, FOR TYPE 347 STAINLESS STEEL AND HASTELLOY X AT 1400 F

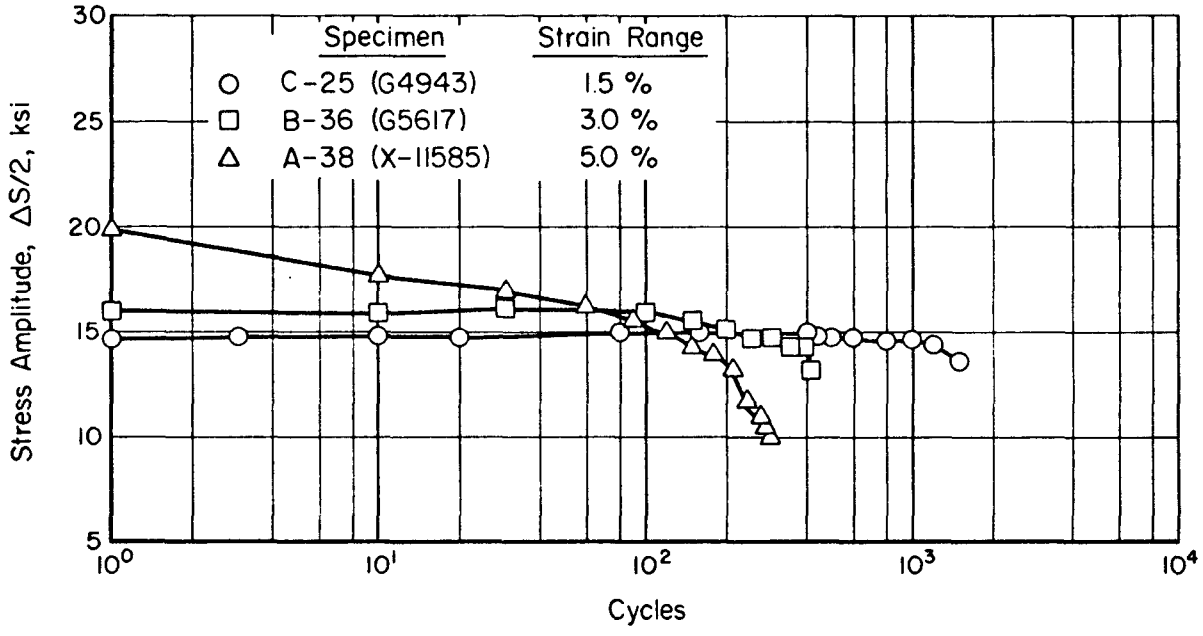

a. Type 347 Stainless Steel

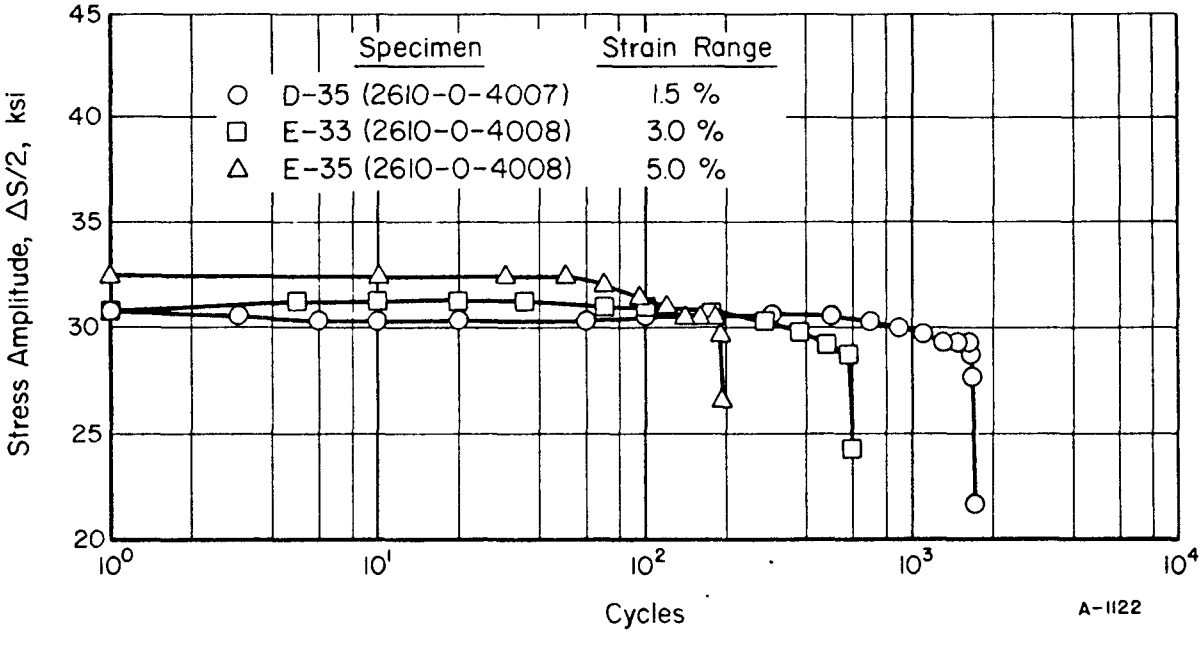

b. Hastelloy X

FIGURE 21. STRESS AMPLITUDE, $\Delta S/2$, VERSUS FATIGUE LIFE, N_f, FOR TYPE 347 STAINLESS STEEL AND HASTELLOY X AT 1600 F

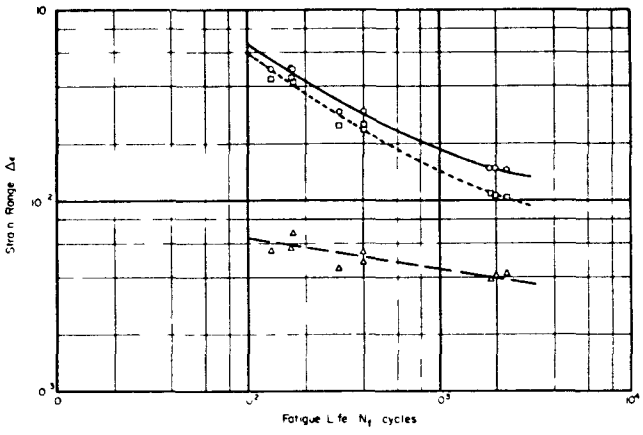

a. Type 347 Stainless Steel Heat X-11585; Series A

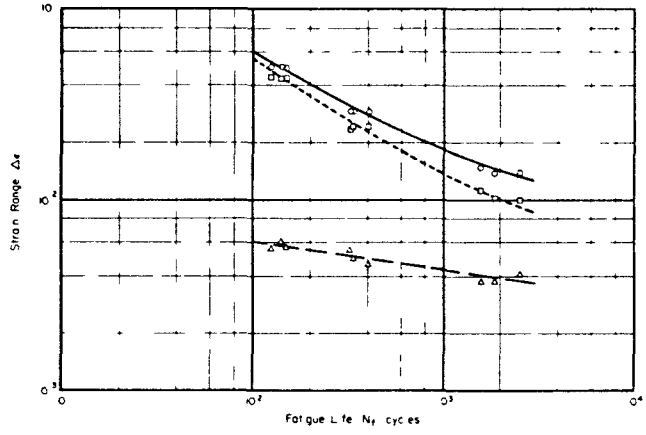

b. Type 347 Stainless Steel Heat G5617; Series B

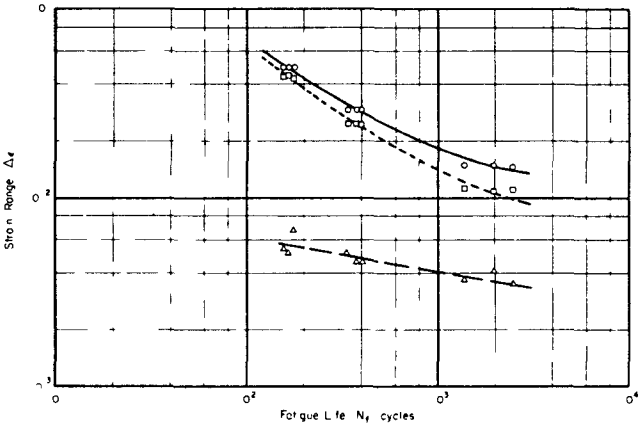

c. Type 347 Stainless Steel Heat G4913; Series C

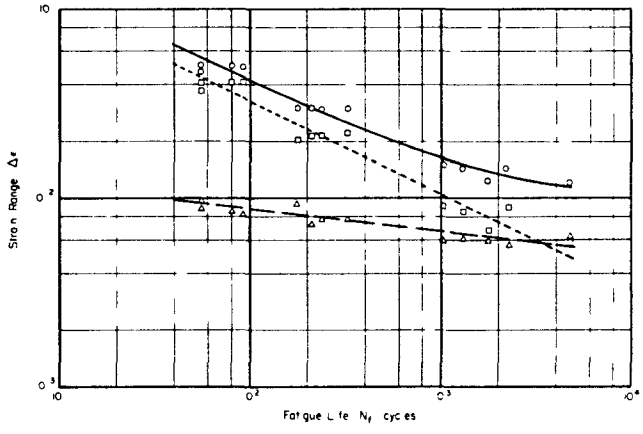

d. Hastelloy X Heat 2610-0-7007; Series D

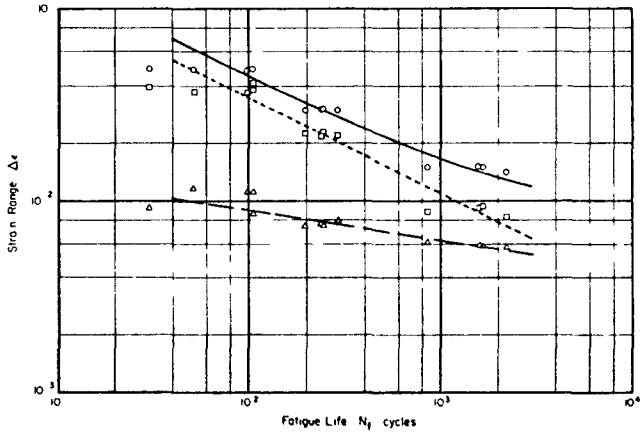

e. Hastelloy X Heat 2610-0-4008; Series E

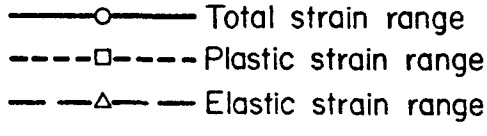

A-1117

FIGURE 22. FATIGUE LIFE, N_f, AS A FUNCTION OF STRAIN RANGE, $\Delta\epsilon$, FOR TYPE 347 STAINLESS STEEL AND HASTELLOY X AT 1000 F AND AT A STRAIN RATE OF 10^{-3} SEC^{-1}

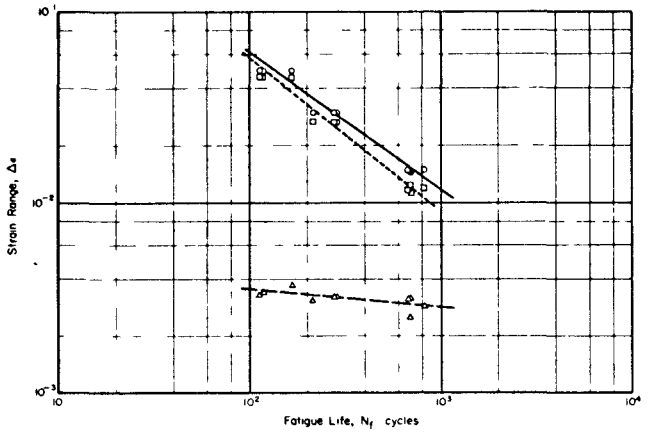

a. Type 347 Stainless Steel Heat X-11585; Series A

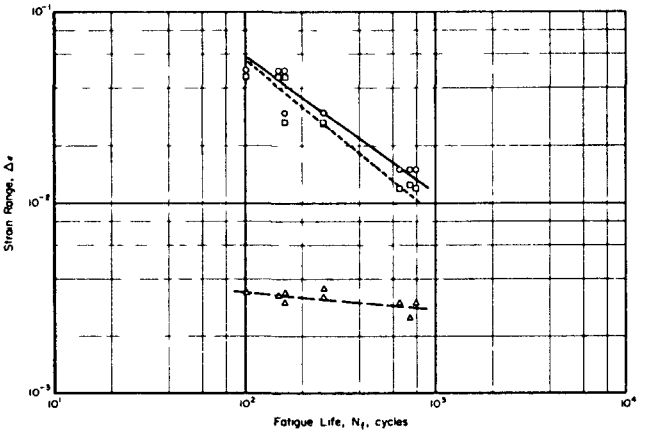

b. Type 347 Stainless Steel Heat G5617; Series B

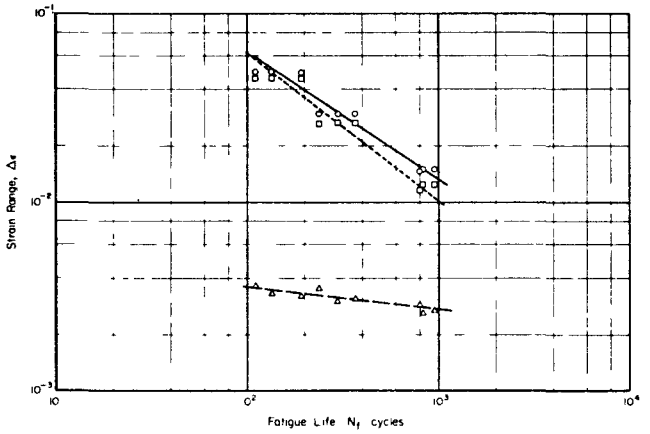

c. Type 347 Stainless Steel Heat G4913; Series C

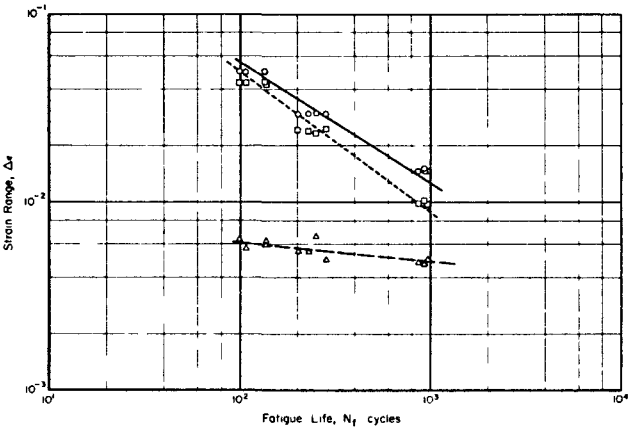

d. Hastelloy X Heat 2610-0-7007; Series D

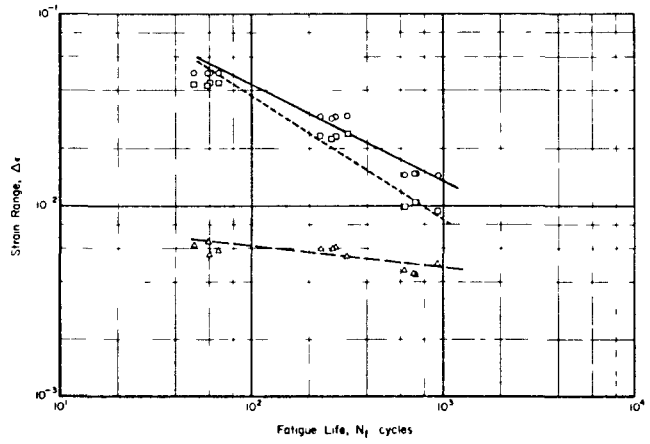

e. Hastelloy X Heat 2610-0-4008; Series E

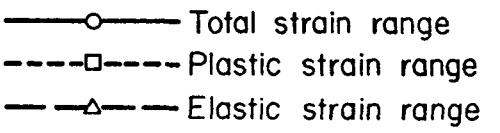

A-1118

FIGURE 23. FATIGUE LIFE, N_f, AS A FUNCTION OF STRAIN RANGE, $\Delta\epsilon$, FOR TYPE 347 STAINLESS STEEL AND HASTELLOY X AT 1400 F AND AT A STRAIN RATE OF 10^{-3} SEC^{-1}

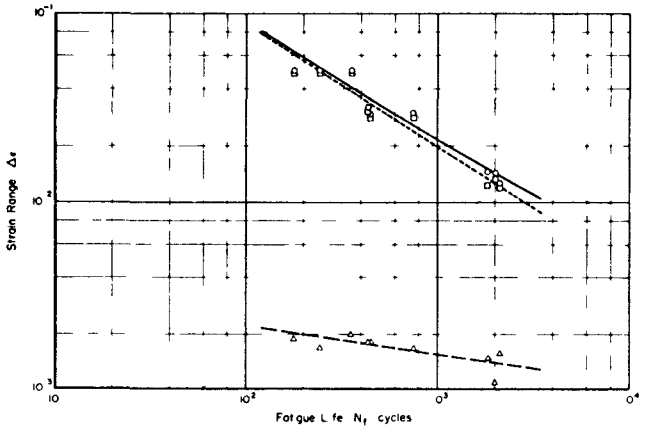

a. Type 347 Stainless Steel Heat X-11585; Series A

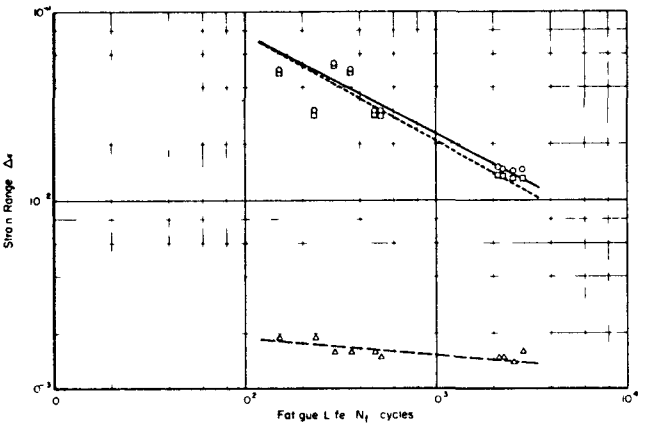

b. Type 347 Stainless Steel Heat G5617; Series B

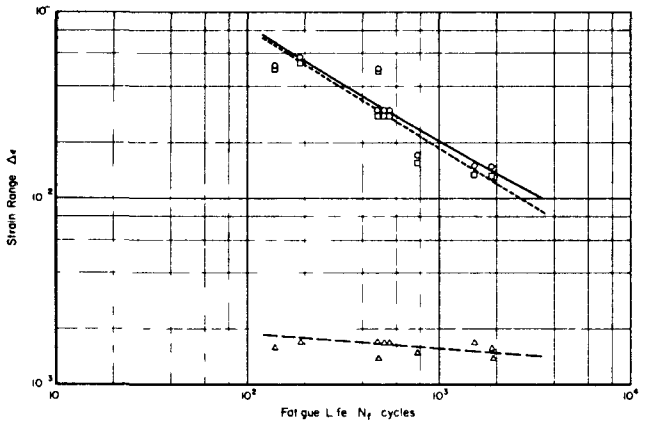

c. Type 347 Stainless Steel Heat G4913; Series C

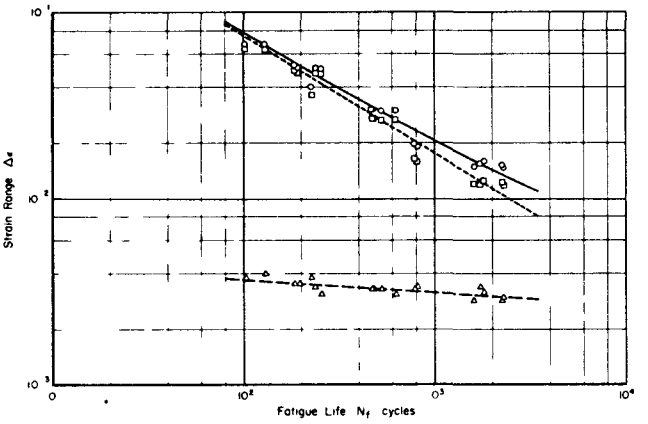

d. Hastelloy X Heat 2610-0-7007; Series D

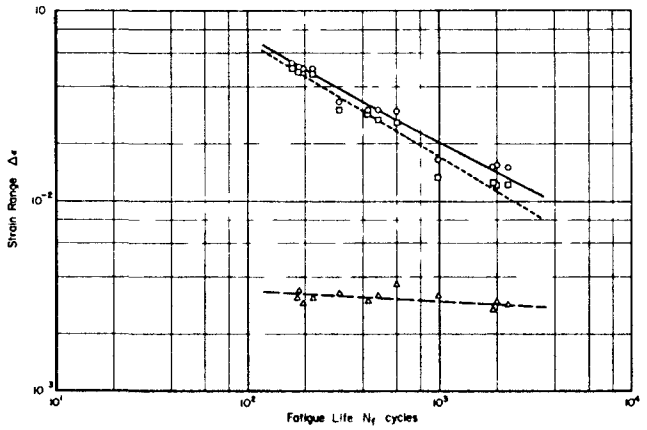

e. Hastelloy X Heat 2610-0-4008; Series E

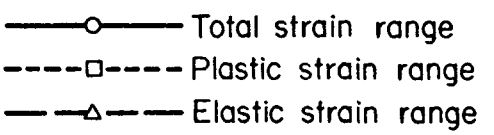

A-1119

FIGURE 24. FATIGUE LIFE, N_f, AS A FUNCTION OF STRAIN RANGE, $\Delta\epsilon$, FOR TYPE 347 STAINLESS STEEL AND HASTELLOY X AT 1600 F AND AT A STRAIN RATE OF 10^{-3} SEC^{-1}

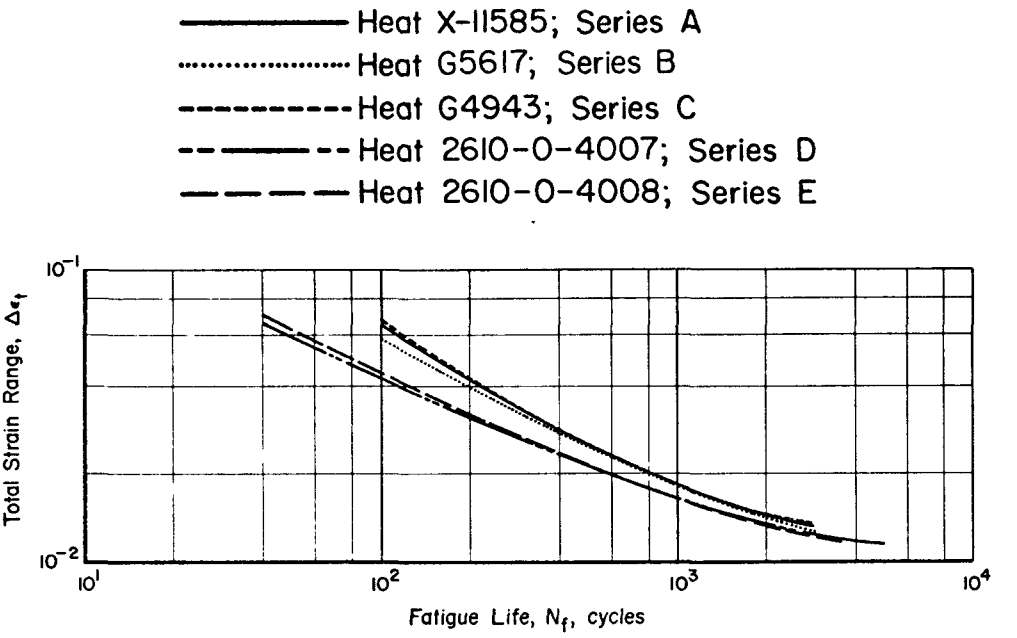

a. 1000 F

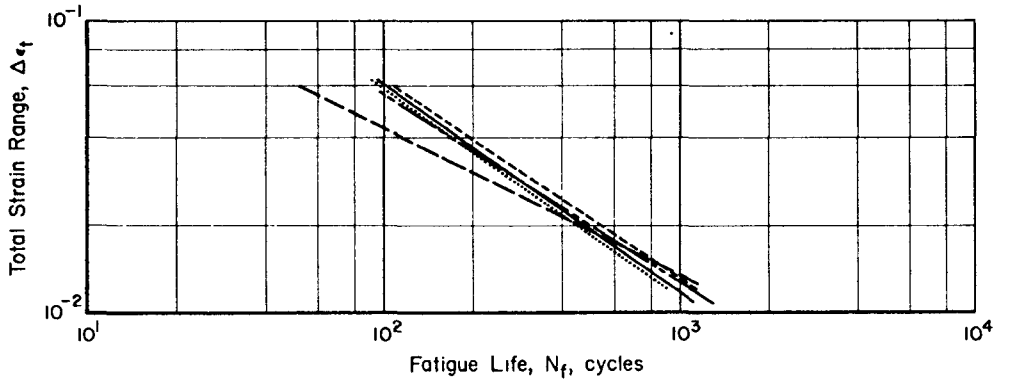

b. 1400 F

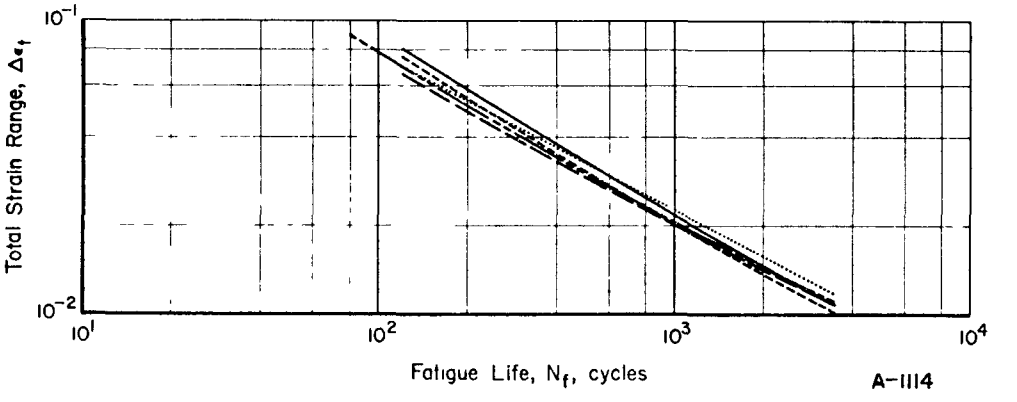

c. 1600 F

FIGURE 25. FATIGUE LIFE, N_f, VERSUS TOTAL STRAIN RANGE, $\Delta\epsilon_t$, FOR TYPE 347 STAINLESS STEEL AND HASTELLOY X AT ELEVATED TEMPERATURE AND AT A AXIAL STRAIN RATE OF 10^{-3} SEC^{-1}

range is the parameter of most importance. Figure 26 shows the total strain range versus fatigue life as an average of the heats from each material. The superimposed curves were averaged when it was believed the results showed a small enough heat-to-heat variation to be considered only as experimental scatter and not a definite trend. The data developed from each temperature group are plotted here to allow direct comparison of the effect of temperature on each of the materials in the program. In addition to the test results for a hydrogen atmosphere, the baseline data (at 1400 F and in air) are plotted on this graph to show the effect of the hydrogen environment on the fatigue life.

The fatigue curves for all five heats of material at 1000 F are presented in Figure 22. On these logarithmic coordinates, the elastic strain range curves for both materials and the plastic strain range curves of the Hastelloy X were well approximated by straight lines for the range of available data. The plastic strain range curves for the Type 347 stainless steel and all of the total strain range curves were best described by curved lines that are concave upward. Examination of Figure 25(a) shows that both materials gave repeatable results among their respective heats at 1000 F. However, the fatigue lives of Type 347 stainless steel and Hastelloy X were considerably different at the 5.0 percent strain range. This trend is to be expected since Type 347 stainless steel had slightly better ductility than the Hastelloy X at 1000 F. The fatigue lives of both materials tended to converge at the 1.5 percent strain range as ductility tends to be less of a factor in the fatigue life as strain range decreases.

Results for all five heats at 1400 F are plotted in Figure 23. Over the range of available data, all of the total, plastic, and elastic strain-range curves are essentially linear on logarithmic coordinates. As seen in Figure 25(b), the material for all heats of Type 347 stainless steel and the material from Series D of Hastelloy X show fatigue lives which are almost identical. Only the Series E of Hastelloy X has a slightly lower fatigue life curve at the higher strain ranges. This heat-to-heat variation in fatigue life of the Hastelloy X is related to the variation of the true fracture ductility between two heats. The true fracture ductility of Series D

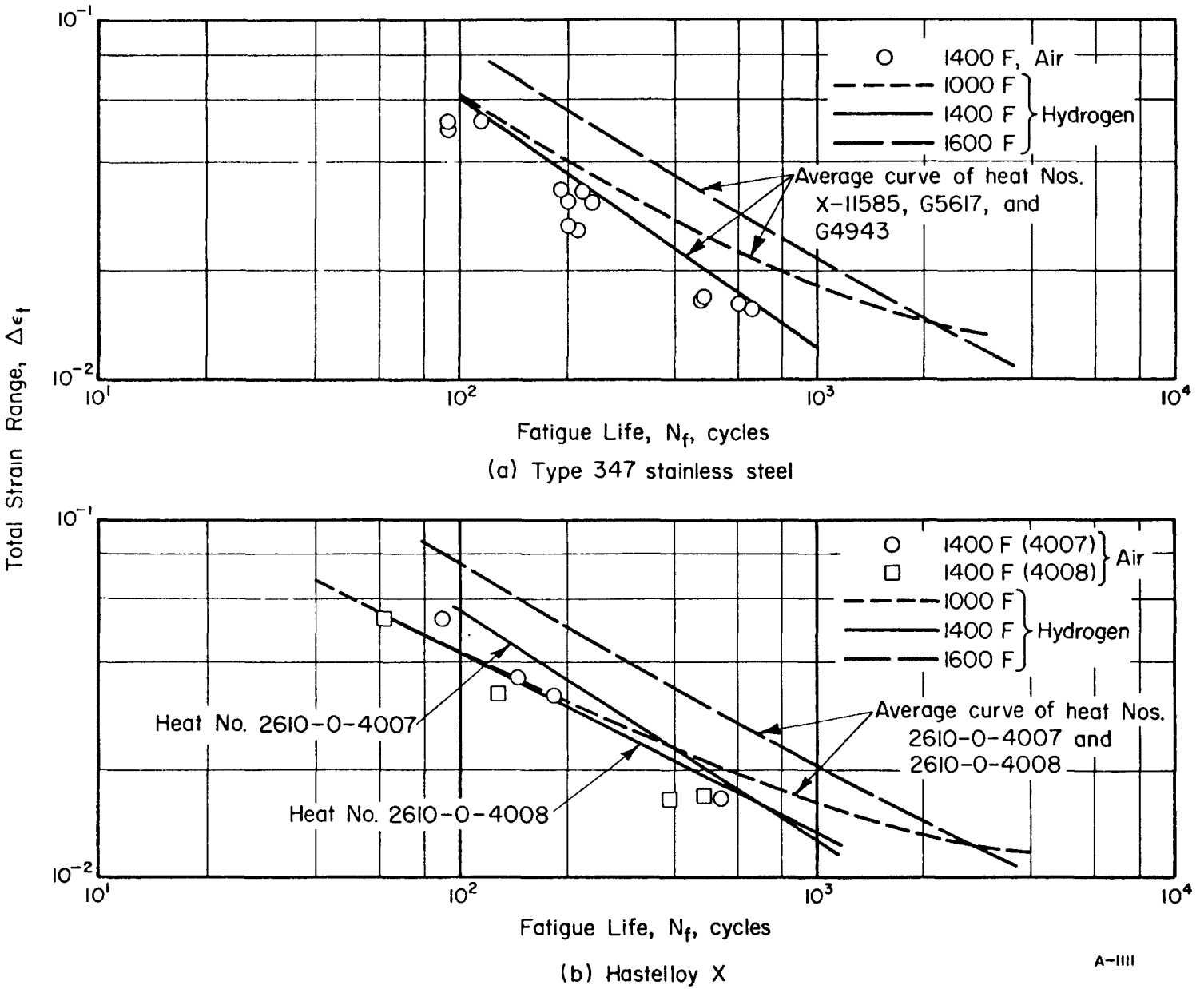

FIGURE 26. COMPARISON OF FATIGUE LIFE, N_f, AT 1000, 1400 AND 1600 F AND A STRAIN RATE OF 10^{-3} SEC^{-1}

material was higher than that of the Series E material; hence, the material with greater ductility showed better fatigue resistance at high strain ranges. This behavior is in contrast to that at 1000 F where the two heats of Hastelloy X have similar true fracture ductilities and, as a result, the fatigue lives of the two heat were almost identical.

Figure 24 shows the logarithmic plots of fatigue curves for all five heats of material at 1600 F. The elastic and plastic strain-range curves are represented by straight lines and the total strain-range curves have a slightly concave-upward curvature. The data for the three heats of Type 347 stainless steel [Figures 24(a), 24(b), and 24(c)] showed a great amount of scatter, particularly at the 5 percent strain range. In contrast to the Type 347 stainless steel, the data obtained from the two heats of Hastelloy X exhibited very little scatter [Figures 24(d) and 24(e)]. When the plots of total strain range versus fatigue life are superimposed [Figure 25(c)], it is seen that all five heats of material have fatigue lives which are almost identical.

Figure 26 is a comparison of the fatigue behavior of each material at the three test temperatures. Where it was considered reasonable, the curves for each heat of a particular material were averaged. Throughout most of the strain range (approximately 1.5 to 5.0 percent), the fatigue lives of both materials at 1600 F were superior to the lives at either 1000 F or 1400 F. However, near 1.5 percent at 1000 F, the fatigue lives of both Hastelloy X and Type 347 stainless steel are improved over those at 1600 F. This is due to the sharp "knee" in the 1000 F curves. Compared to the fatigue lives at 1000 F and 1600 F, both materials displayed the worst fatigue characteristics at 1400 F.

In addition to the low-cycle fatigue data obtained from the tests conducted in the hydrogen atmosphere, the low-cycle fatigue data for those tests conducted in air at 1400 F (see Table 4) are also plotted on this graph. The fatigue life of the Type 347 stainless steel appeared to be slightly improved when the tests were run in hydrogen [see Figure 26(a)]. In contrast, the hydrogen environment appeared to have little effect on the fatigue life of the Hastelloy X. Only at the low strain range, 1.5 percent, did the results in hydrogen appear improved over the results in air [see Figure 26(b)]

CONCLUSIONS

As a result of this experimental program, significant observations were made concerning the cyclic hardening and/or softening behavior, and the low-cycle fatigue resistance of Type 347 stainless steel and Hastelloy X in hydrogen gas environment at 1000, 1400, and 1600 F.

The observations on cyclic hardening and/or softening behavior are listed below:

- At 1000 F, both alloys showed significant cyclic hardening at strain ranges between 1.5 and 5.0 percent. The Hastelloy X hardened more than the Type 347 stainless steel.
- Over the same strain ranges at 1400 F, the Type 347 stainless steel exhibited only a slight tendency to cyclically harden; the Hastelloy X hardened significantly with a greater amount of cyclic hardening at 5.0 percent than at 1.5 percent strain range.
- Over the same strain ranges at 1600 F, both alloys did not cyclically harden. The Hastelloy X was cyclically stable at strain ranges between 1.5 and 5.0 percent. The Type 347 stainless steel was cyclically stable at 1.5 and 3.0 percent strain ranges and cyclically softened at the 5.0 percent strain range.

The observations relative to the low-cycle fatigue resistance of the materials are listed below:

- At strain ranges above 1.5 percent, both alloys had greater fatigue life at 1600 F than at either 1000 or 1400 F.
- At 1.5 percent strain range, both alloys had greater fatigue life at 1000 F than at either 1400 or 1600 F.
- At strain ranges between 1.5 and 5.0 percent. both alloys showed the lowest fatigue life at 1400 F (compared to 1000 and 1600 F).

- At 1000 F, the Type 347 stainless steel had greater fatigue resistance than the Hastelloy X at strain ranges of 3.0 and 5.0 percent, while both materials had about the same fatigue resistance at a strain range of 1.5 percent.
- At 1400 F, all three heats of the Type 347 stainless steel and Heat 2610-0-4007 of the Hastelloy X had about the same fatigue resistance. However, Heat 2610-0-4008 of the Hastelloy X had a lower fatigue resistance than the other four heats of material at strain ranges of 3.0 and 5.0 percent.
- At 1600 F, all five heats of material had essentially the same fatigue resistance for strain ranges between 1.5 and 5.0 percent.

Based on the results of this program, the Type 347 stainless steel has low-cycle fatigue resistance superior to that of the Hastelloy X. This conclusion is based on the fact that when a significant difference in low-cycle fatigue life existed between the two alloys, the Type 347 stainless steel had greater fatigue lives than the Hastelloy X at comparable total strain ranges. Other operational variables, such as hold time or environment, may affect the low-cycle fatigue resistance and conceivably influence the selection of a material for this application.

REFERENCES

1. Slot, T., Stentz, R. H., and Berling, J. T., "Controlled-Strain Testing Procedures", Manual on Low-Cycle Fatigue Testing, ASTM-STP-465, American Society for Testing and Materials, Philadelphia, pp 27-66 (1969).

2. Feltner, C. E., and Mitchell, M. R., "Basic Research on the Cyclic Deformation and Fracture Behavior of Materials", Manual on Low-Cycle Fatigue Testing, ASTM-STP-465, American Society for Testing and Materials, Philadelphia, pp 27-66 (1969).

3. Morrow, JoDean and Tuler, F. R., "Low Cycle Fatigue Evaluation of Inconel 713C and Waspaloy", Transactions, American Society of Mechanical Engineers, Series D, Journal of Basic Engineering, Vol. 87, No. 2, pp 275-289 (June, 1965).